



Calhoun: The NPS Institutional Archive

DSpace Repository

Theses and Dissertations | 1. Thesis and Dissertation Collection, all items

1968-03

An investigation of penetration and spreading for various fluids injected into a supersonic stream

Castle, Robert Wellington

Monterey, California: U.S. Naval Postgraduate School

http://hdl.handle.net/10945/28315

Downloaded from NPS Archive: Calhoun



http://www.nps.edu/library

Calhoun is the Naval Postgraduate School's public access digital repository for research materials and institutional publications created by the NPS community. Calhoun is named for Professor of Mathematics Guy K. Calhoun, NPS's first appointed -- and published -- scholarly author.

Dudley Knox Library / Naval Postgraduate School
411 Dyer Road / 1 University Circle
Monterey, California USA 93943

AN INVESTIGATION OF PENETRATION AND SPREADING FOR VARIOUS FLUIDS INJECTED INTO A SUPERSONIC STREAM

by

Robert Wellington Castle, Jr.

UNITED STATES
NAVAL POSTGRADUATE SCHOOL



THESIS

AN INVESTIGATION OF PENETRATION

AND SPREADING FOR VARIOUS FLUIDS INJECTED

INTO A SUPERSONIC STREAM

by

Robert Wellington Castle, Jr.
Lieutenant, United States Navy

March 1968

This document is subject to special export controls and each transmittal to foreign governments or foreign nationals may be made only with prior approval of the U. S. Naval Postgraduate School.

LIBRARY
NAVAL POSTGRADUATE SCHOOL
MONTEREY, CALIF. 93940

AN INVESTIGATION OF PENETRATION AND SPREADING FOR VARIOUS FLUIDS INJECTED INTO A SUPERSONIC STREAM

by

Robert Wellington Castle, Jr.
Lieutenant, United States Navy
B.S., Rensselaer Polytechnic Institute, 1959

Submitted in partial fulfillment of the
requirements for the degree of

MASTER OF SCIENCE IN AERONAUTICAL ENGINEERING

from the

NAVAL POSTGRADUATE SCHOOL
March 1968

Thesis
C.1

ABSTRACT

A study was conducted to determine the effects of varying the fluid properties of viscosity, surface tension, and density on liquid jet breakup, penetration, and spreading. Water, heptane, and a 58 per cent glycerin-42 per cent water mixture (by mass) were injected transversely into Mach 2.8 and 4.0 airstreams through various circular orifices located in the surface of a flat plate model. Experiments were performed with injector orifices varying in diameter from 0.0145 inches to 0.080 inches, using injectant total pressures ranging from 30 psia. to 3000 psia. Steady-state penetration and lateral spreading distances were measured from scattered light photographs, and qualitative analyses of shock waves induced by the liquid jet were made using schlieren photographs.

A non-dimensional penetration parameter ($M_\infty h/d_e$) was found to be dependent on the ratio of the injection total pressure to the free stream static pressure, but not on a variation of fluid injectant properties of surface tension, viscosity, and density.

Lateral spreading was determined to be a function primarily of the orifice diameter, with weak dependence upon the injection pressure ratio. Changing the injectant fluid properties of surface tension, viscosity, and density had no noticeable effect on lateral spreading. Within experimental accuracy, spreading was also considered to be Mach number independent.

LIBRARY
NAVAL POSTGRADUATE SCHOOL
MONTEREY, CALIF. 93940

TABLE OF CONTENTS

SECTION		PAGE
I.	INTRODUCTION	11
II.	EXPERIMENTAL EQUIPMENT	14
III.	TEST PROCEDURES	18
IV.	DATA REDUCTION	22
V.	DISCUSSION	25
VI.	CONCLUSIONS	35
REFERENCES		36
TABLES		40
FIGURES		52
DISTRIBUTION LIST		71

LIST OF TABLES

NUMBER		PAGE
I.	Injector Characteristics	40
II.	Liquid Injectant Properties	41
III.	Summary of Data and Calculated Values at M = 2.8	42
IV.	Summary of Data and Calculated Values at M = 4.0	47

LIST OF FIGURES

FIGURE PAGE

1. Flat plate model used to obtain penetration data 52
2. Layout of the flat plate model used to obtain penetration data 53
3. Flat plate model used to obtain lateral spreading data 54
4. Cross-section of an injector 55
5. Schematic diagram of the liquid injection system installation 56
6. Photograph of the wind tunnel and injection system installation 57
7. Schematic diagram of the optical system 58
8. Photograph of the installation of the penetration flat plate model 59
9. Photograph of the installation of the lateral spreading flat plate model 59
10. Penetration with various orifices injecting water into Mach number 2.8 and 4.0 cross flows 60
11. Penetration with various orifices injecting heptane and glycerin into Mach number 2.8 and 4.0 cross flows 61
12. Penetration of heptane, glycerin, and water injected forward into Mach number 2.8 and 4.0 cross flows at injection angles of 5°, 20°, and 30° measured from the normal 62
13. Lateral spreading with various orifices injecting water, heptane, and glycerin into Mach number 2.8 and 4.0 cross flows 63

FIGURE PAGE

14. Run number 1-3 64

15. Run number 1-4 64

16. Run number 1-5 65

17. Run number 1-6 65

18. Run number 1-7 66

19. Run number 1-8 66

20. Enlarged schlieren photograph of injector 2 with water injection in a Mach number 2.8 cross flow 67

21. Schlieren photograph of the flow field around a 0.125 inch diameter cylinder in a Mach number 2.8 cross flow 67

22. Run number 1-44 68

23. Run number 1-40 68

24. Run number 2-1 69

25. Run number 2-3 69

26. Run number 2-4 70

27. Run number 1-32 70

28. Run number 1-33 71

29. Run number 1-34 71

30. Run number 1-65 72

31. Run number 1-70 72

32. Run number 1-73 73

TABLE OF SYMBOLS

C	Constant of the penetration equation
d_e	Equivalent orifice diameter (in.)
d_o	Orifice diameter (in.)
h	Penetration height (in.)
l	Distance downstream from orifice (in.)
L	Injector orifice length (in.)
$\dot{m}$	Mass flow rate (gms. mass/sec.)
M_∞	Free stream Mach number
P_1	Free stream static pressure (psia.)
P_{oj}	Injection total pressure (psia.)
P_{ot}	Free stream total pressure (psia.)
T_1	Free stream static temperature (°R.)
W	Lateral spreading width (in.)
ρ_1	Injectant fluid density (lb. mass/ft.^{3})
α	Exponent of the extrapolation equation
β	Exponent of the penetration equation
l/d_e	Non-dimensional distance downstream from the injector orifice
L/d	Orifice length-to-diameter ratio
$M_\infty h/d_e$	Non-dimensional penetration parameter
P_{oj}/P_1	Non-dimensional injection pressure ratio
W/d_e	Non-dimensional lateral spreading parameter
h/d_e	Non-dimensional penetration height

ACKNOWLEDGMENTS

The writer wishes to express his sincere appreciation to Drs. K. P. Horn and M. A. Kolpin of the Plasma Research Laboratory, Aerospace Corporation, El Segundo, California, and to Professor R. E. Reichenbach of the Naval Postgraduate School, Monterey, California, for their assistance in providing the flat plate models and injectors in support of this research effort and for access to their data and pre-publication copy of their investigation as fundamental background material. Other people who contributed directly to the successful completion of this thesis were Mr. Ted Dunton and Mr. Norman Leckenby of the Naval Postgraduate School Department of Aeronautics and the personnel of the Department of Aeronautics Metal Shop. Their genuine interest and helpful suggestions were deeply appreciated.

The writer is particularly indebted to his thesis advisor, Dr. R. E. Reichenbach, for his guidance of this research effort.

I. INTRODUCTION

Numerous investigations have been conducted in recent years on the secondary injection of a fluid jet into a supersonic cross stream. Research into the effects of secondary injection have generally proceeded in either of two directions: (1) studies of the interaction of secondary injection with the free stream and the resulting pressure field around and aft of the jet which produces side forces on a body and (2) consideration of the characteristics of the jet breakup on penetration and spreading, droplet distribution, and mixing. Detailed information and understanding of liquid jets injected into supersonic streams could prove valuable in the areas of re-entry communications (Refs. 1-6), supersonic combustion ram jets (Refs. 7-12), thrust vector control (Refs. 13-21), and external vehicle control (Refs. 22-23).

In thrust vector control and re-entry vehicle control, the shock system induced by secondary liquid injection is closely related to the characteristics of the liquid jet itself. Liquid jets using chemically reactive fluids are being considered for the above applications. Not only is information on the jet required, but additional information on the shock system is necessary to determine the side forces generated.

One possible solution for the re-entry communications blackout presently occurring with lifting re-entry vehicles is to form a "window" in the plasma sheath over the communications antenna by injecting a liquid coolant. A mixture of a coolant containing an electronegative species may reduce the electron concentration to an acceptable level for maintaining continuous communications. System studies (Ref. 1) indicate that a small mass flow rate is required for cooling; therefore, a very high injection pressure would be required to achieve sufficient

penetration through the desired small orifices. Necessary information for using a coolant injectant technique includes the spatial distribution and droplet size of the resulting spray. This information is required to estimate the evaporation rate and hence the cooling rate of the ionized gas.

In the area of supersonic combustion preliminary investigations indicate that the method of fuel injection influences supersonic mixing, and experimental evidence (Ref. 24) indicates that the fuel mixing is enhanced by cross stream injection. Since mixing must occur on a molecular scale to achieve efficient combustion, information on liquid jets would be valuable here also.

The practical aspects of liquid or gaseous injection into a supersonic stream are well established by numerous experimental studies; however, the complex interaction between the secondary injectant and the primary flow is not well understood and is not readily amenable to theoretical analysis. Nevertheless, many approximate analytical solutions for predicting the induced side forces have been generated (Refs. 18, 25-28). Most of the published work is concerned with gaseous injection and relatively little work (Refs. 11, 15, 19, 32, 33) has been devoted to an analytical study of liquid injection. This is primarily due to the fact that the processes of liquid atomization, evaporation, jet penetration, and mixing are difficult to analyze concurrently. Moveover, another significant parameter for determining the behavior of a specific liquid injectant is the vapor pressure of the liquid, relative to the pressure it encounters during the injection process. Therefore, future improvements in re-entry communications, thrust vector control, and re-entry vehicle control will require generation of additional experimental data on jet penetration, spreading, and droplet spatial distribution.

Liquid injection into still or subsonic flows has been studied in depth (Refs. 34-37). Most of this work was motivated by compression ignition engines, liquid propellant rockets, or by sprays in chemical processes. Studies of injection of a liquid jet into a transverse supersonic stream have provided only limited experimental data (Refs. 11, 12, 23, 33, 39). The basic goal of recent investigations has been to obtain additional information concerning the processes of interaction and the associated forces caused by secondary injection and, in particular, to determine similarity rules for the important parameters as in Ref. 38.

This paper is an experimental study of jet breakup, penetration, and spreading of various liquids injected into a supersonic flow. The parameters investigated were grouped into three general areas: (1) the injector, (2) the liquid injectants, and (3) the supersonic primary flow. Injector characteristics were specified by the orifice diameter, orifice length-to-diameter ratio, injection angle, and injection total pressure. Fluid injectant parameters included surface tension, viscosity, and density. The supersonic main stream was characterized by the total and static free stream pressures, Mach number, density, and viscosity.

II. EXPERIMENTAL EQUIPMENT

A series of experiments were conducted in the 4 inch by 4 inch supersonic wind tunnel at the Naval Postgraduate School, Monterey, California, in which water, heptane, and a 58 per cent glycerin-42 per cent water mixture (by mass) were injected through various orifices located in the surface of a flat plate model. Experiments were conducted at test section Mach numbers of 2.8 and 4.0, with free stream stagnation pressure ranges of 45 to 120 psia. for Mach 2.8 flow and 135 to 210 psia. for Mach 4.0 flow. The experimental data consisted of free stream static and stagnation pressures, injection total pressures, and still photographs of the liquid jet penetration and spreading using schlieren and scattered light optical techniques.

Two stainless steel flat plates with sharp leading edges were used to obtain penetration and lateral spreading data. The surface of the plate which contained the injector orifice was parallel to the free stream. The flat plate shown in Fig. 1 was used to observe penetration. It had interchangeable injectors and eight static pressure orifices located in the surface downstream of the injector as shown in the schematic diagram of Fig. 2. The liquid injectant passed through one forward mount into the injector, and four pressure leads were located in each aft mount. The flat plate model in Fig. 3 used to observe lateral spreading had the same dimensions as the penetration plate. It was attached to a circular base by three mounts so it could be inserted directly into the tunnel in place of one of the observation windows. The liquid injectant was passed through the base directly into the rear of the injector in the spreading plate to minimize rotational flow of the fluid.

A sketch of an injector is shown in Fig. 4, and the characteristics of the injectors used during the investigation are listed in Table I. The injector plenum was designed as large as possible to insure that the ratio of plenum chamber velocity to orifice exit velocity would be relatively small. Thus it could be assumed that the pressure drop took place across the orifice alone. An L/d_o ratio of four was considered optimum to maximize the orifice coefficient and keep the viscous losses to a minimum. Since the maximum injector length was 0.5 inch, the plenum chamber size requirement necessitated some variation in the L/d_o for the larger orifices. With large orifices the assumption that $V_{plenum}/V_{orifice}$ was very small may not be entirely valid. The axis of some injector orifices was inclined to the free stream at angles measured from the normal to the surface of the flat plate. The injectors were machined to allow both upstream and downstream injection. Leakage was prevented by two "O" ring seals on the injector body and a steel backing plate with an "O" ring seal retained by two steel cap screws.

A schematic diagram of the liquid injectant supply system is shown in Fig. 5 and Fig. 6 is a photograph of the installation. A 6000 psi, 4.4 cubic foot gaseous nitrogen bottle controlled by a Benbow pressure regulator provided pressurization of the 500 cubic centimeter accumulator. The injectant total pressure, measured by a Bourdon-type pressure gage upstream of the injector, was varied from 30 to 3000 psig. Three pressure gages with ranges of 0-100, 0-800, and 0-5000 psig, were used as required to provide accurate measurement of the injectant pressures. Fluid flow through 0.25 inch stainless steel tubing to the injector was controlled by a Hoke control valve located between the accumulator and the flat plate.

Water, heptane, and a 58 per cent glycerin-42 per cent water mixture (by mass) were the three injectants used in the series of experiments to investigate the effects of varying the fluid properties of viscosity, surface tension, and density on penetration, spreading, and jet breakup. Fluid properties are listed in Table II. Water was used as the liquid injectant in a majority of the runs. Heptane was considered representative of low surface tension fluids, and the glycerin-water mixture was used as it had a viscosity an order of magnitude higher than that of water.

Figure 7 is a schematic diagram of the optical system used for observation and photography of the jet spray and its associated shock system. A schlieren optical system was used to observe the shock system in the primary flow associated with liquid injection. The double mirror folded axis system incorporated a General Electric BH6 mercury arc lamp source, two 100 inch focal length 8 inch diameter spherical mirrors, and two 9 by 15 inch plane mirrors. Two 300 watt photo floodlights mounted in a light bar and placed downstream of the test section provided illumination of the jet spray. Light scattered by the liquid droplets was reflected through part of the schlieren mirror system and was photographed simultaneously with the shock waves.

Composite pictures of the flow field and the jet penetration were found to incorrectly indicate a reduced spray pattern. The schlieren light rays traversed the less dense outer spray regions almost unaffected due to the low concentration of liquid droplets at the outer edges, and the scattered light reflected by the droplets could not be distinguished. Therefore, data for normal penetration and lateral spreading were obtained using only scattered light.

All static pressures and the free stream total pressures less than 100 psia. were measured with Statham pressure transducers mounted in a Cox digital readout system. The transducers were available with full scale ranges of 1.5, 15, and 100 psia., enabling expected pressure ranges to be matched with the proper transducer to reduce measurement error to within $\pm$ 1 per cent. A Bourdon-type dial gage with a range of 0-300 psig. was used when the free stream total pressure exceeded 100 psi. The liquid injectant total pressure was measured by a Bourdon-type dial gage with a range of 0-5000 psig. to an accuracy of within $\pm$ 2 per cent.

III. TEST PROCEDURES

During the study the velocity of the tunnel free stream was constant at each Mach number since the free stream stagnation temperature was approximately 530 °R. Therefore the static temperatures over the flat plate were 206 °R. at Mach number 2.8 and 126 °R. at Mach number 4.0. The three liquid injectants were initially at a temperature of approximately 530 °R. in the accumulator. The temperature of the fluids at the injector orifice was not measured.

Prior to starting the test runs the injector orifices were calibrated by timing the actual mass flow of each fluid through the orifices under a pressure differential of 800 psi. and calculating an "equivalent orifice diameter" (d_e) using the continuity equation and the incompressible Bernoulli's equation. Assuming the injector plenum velocity negligible, d_e was expressed as

$$d_e = 0.0607 \sqrt{\frac{\dot{m}_m}{P_{oj}\,\rho_j}} \qquad (1)$$

Although the mass flow rates varied slightly for the three fluids injected through each injector orifice at the same pressure, the calculated equivalent diameters were very nearly equal, suggesting little variation in frictional or viscous losses through the orifice. Therefore the d_e for each orifice was considered constant throughout the study.

A typical penetration run proceeded in the following manner. The "O" ring seals of the selected injector were carefully checked before the injector was inserted into the plate to prevent leakage at

high injection pressures. The flat plates were mounted in the tunnel as shown in Figs. 8 and 9. The schlieren system alignment was checked on the leading edge of the plate, and the proper focus was obtained by placing a small drill bit on the plate centerline and then adjusting the filmback to the desired image plane of the test section. Kodak neutral density filters were used in the schlieren system when making composite photographs to reduce the intensity of the BH6 source and heighten the contrasting scattered light reflected by the solid jet and the droplets resulting from jet breakup.

The accumulator was filled and pressurized with gaseous nitrogen to slightly above the desired injection pressure to allow for a pressure drop across the regulator when initiating injection. Typical focal plane shutter speeds of 1/100 to 1/125 seconds were set for Polaroid Type 52 film, and the lighting system was actuated. The tunnel was started, and the pressure was increased to the desired free stream stagnation pressure. At steady-state free stream conditions the Hoke liquid injectant cutoff valve was opened and a steady liquid jet spray pattern established. The photograph and pressure readings were then taken simultaneously, and the tunnel was secured.

Tests for lateral spreading involving the vertically mounted flat plate required relatively simple changes to the supporting optical and liquid injection systems. The tubing connection from the plate to the liquid injectant cutoff valve was replaced, the desired injector inserted into the plate, and the plate mounted in one wall of the tunnel. The opposite window was changed to a solid glass window. Since the spreading plate was designed to provide a reflecting surface for schlieren photography when required, care was taken during installation

not to mar the surface. The focus was adjusted to provide a clear picture of the spreading while keeping the plate surface slightly out of focus, since small amounts of the liquid injectant entered the boundary layer and interfered with proper visualization of the injectant jet spreading boundaries.

Normally, three runs were made at each injection pressure setting. The three fluids were injected sequentially through the same orifice in order to maintain constant free stream and injector pressure conditions. The accumulator was purged with dry nitrogen prior to filling with each new fluid.

The orifice size directly affected the length of injection time using the 500 cubic centimeter accumulator. The smaller injectors A, X, and Double permitted injection up to 45 seconds, while the larger injectors 1 through 6 were generally limited to a maximum of 15 seconds. Runs were also limited by accumulated ice buildup on the aft section of the plate due to the low free stream static temperatures, especially during water injection.

Penetration data at Mach 2.8 were obtained with three liquids utilizing all injectors except injector number 5. At Mach 4.0 injectors A, B, 1, 2, and 6 were considered sufficient to cover the injector diameter range.

Spreading data were limited to injectors A, Double, and 2 for the three fluids at Mach 2.8 and to A, B, and 2 injecting water at Mach 4.0. The free stream stagnation pressures required to allow fluid injection were higher for both Mach numbers than were required during penetration runs. This could possibly be due to more numerous corners and protrusions on the spreading model which caused additional shock

wave interference downstream of the test section. All photographs and data utilized in this thesis for both penetration and spreading studies were considered free of any tunnel interference.

IV. DATA REDUCTION

Considerable attention was focused on obtaining consistent data during the penetration and spreading runs. Prior to attempting runs for data the optical and fluid injection systems were operated to check for proper lighting and to determine maximum allowable injection total pressures. Photographs of these tests were retained for qualitative analyses of flow visualization but were not incorporated into the data presented in this thesis. Photographs taken during fluid injection of glycerin were frequently unusable as the unsteady free stream flow field, which occurred as the normal shock wave moved downstream during tunnel starting, caused the residual injectant fluid to flow from the orifice and be deposited on the windows. Although water and heptane were also deposited on the windows, they evaporated rapidly; but the viscous glycerin required removal and cleaning of the windows before the photographing could continue.

Penetration distances of the liquid jets were measured from 8 by 10 inch enlargements of the Polaroid photographs. The boundary layer growth from the leading edge of the plate to the injector orifice was calculated to be 0.01 inches and was considered negligible. The penetration distance (h) was then measured along a normal from the surface of the flat plate to the outer edge of the jet spray. Each penetration distance was obtained at a measured non-dimensional distance ($1/d_e$) downstream from the injection orifice. The penetration and spreading data in Ref. 38 were presented for an $1/d_e$ of 150. The greater portion of the present data used the larger injectors 1 to 6, where the penetration at a maximum $1/d_e$ of approximately 75 could be obtained directly from the photograph. Thus extrapolation of the

present data was required from an $1/d_e$ of 75 or less, depending on the effective orifice diameter, to 150 in order to present a useful comparison.

An empirical relationship was obtained between the non-dimensional penetration height (h/d_e) and $1/d_e$ of the form

$$(h/d_e) \propto (1/d_e)^{\alpha} \qquad (2)$$

where the exponent α was determined graphically.

The graphical approach to determine the values of the exponent α for various injectors was to plot, on a log-log scale, values of h/d_e measured at several $1/d_e$'s, starting at 25 and progressing in increments of 25, plus an h/d_e measured at the maximum $1/d_e$ obtainable on the photograph. The number of points obtained varied for each injector. The numerical value for the exponent α was calculated from the slope of a straight line drawn through the three points located furthest downstream from the point of injection. α was considered valid only for the limited extrapolation of $1/d_e$'s up to 150. Ranges of the values for α were as follows:

Orifice	Exponent α
1	0.1125 - 0.1240
2,3,4	0.1250 - 0.1550
6	0.1000 - 0.1620

Measured and extrapolated values of the non-dimensional penetration parameter $(M_\infty h/d_e)$, defined as the non-dimensional penetration height times Mach number, are tabulated with the data in Tables III and IV. Graphical presentation of the penetration parameter as a function

of the ratio of the injection total pressure to the free stream static pressure is shown in Figs. 10, 11, and 12, using the symbols listed in Table II.

W, the width of the spray pattern in lateral spreading, was scaled directly from the photographs. The spreading of the jet decreased rapidly to approximately parallel flow for most injectors while still visible on the plate. Even the larger orifices 2 and 6 attained approximately parallel flow; therefore, the extrapolation was not required for spreading data. A non-dimensional spreading parameter, W/d_e, tabulated in Tables III and IV, is presented in Fig. 13 as a function of the ratio of the injection total pressure to the free stream static pressure, (P_{oj}/P_1), using the symbols listed in Table II.

V. DISCUSSION

The penetration data are presented in Figs. 10, 11, and 12. The data used to obtain the best fit curve in Fig. 10 included all points injecting water through the orifices A, B, 1, 2, and 6 normal to the plate at Mach numbers 2.8 and 4.0. The curve obtained in Fig. 10 was then plotted as a reference curve to provide a comparison for the effects of varying the fluid properties by injecting heptane and glycerin through various injectors normal to the plate (Fig. 11), or at forward angles measured from the normal (Fig. 12). The equation relating a non-dimensional penetration parameter, $M_\infty h/d_e$, to the injection pressure ratio, P_{oj}/P_1, obtained in Fig. 10 for the best fit curve of water injected normal to the surface was of the form

$$\frac{M_\infty h}{d_e} = C \left(\frac{P_{oj}}{P_1}\right)^{\beta} . \qquad (3)$$

The equation of the curve obtained from the experimental data is

$$\frac{M_\infty h}{d_e} = 15.7 \left(\frac{P_{oj}}{P_1}\right)^{0.407} , \qquad (4)$$

and the equation obtained in Ref. 38 is

$$\frac{M_\infty h}{d_e} = 6.77 \left(\frac{P_{oj}}{P_1}\right)^{0.51} . \qquad (5)$$

Both curves are shown in Fig. 10 .

The curve in Fig. 10 and equation 4 were considerably influenced by data at low injection pressures (30 to 200 psia.) and large orifices (injectors 1, 2, and 6). Injectors A and B were previously used in Ref. 38 to obtain water penetration data, and similar penetration

parameters were obtained in this study with these two injectors for the injection pressure ratio range of 200 to 2000. Additionally, water injection data points scaled by this writer from photographs contained in Ref. 38 are very close to the curve of equation 4 between the injection pressure ratio range of 200 to 2000 as indicated in Fig. 10.

Another possible reason for the variation in the two curves may be attributed to the inclusion of liquid nitrogen data in Ref. 38. Liquid nitrogen has a higher vapor pressure than water; therefore, flash vaporization of the liquid nitrogen could have influenced the jet breakup and penetration. Since no careful experimentation has been performed to understand the effects of flash vaporization on jet breakup, the importance of this phenomena has not been completely defined.

Therefore, while the curves represented by equations 4 and 5 could fit the data in the intermediate pressure ratio range, equation 4 was considered to more properly characterize a single fluid penetration.

Increasing the Mach number from 2.8 to 4.0 reduced the measured penetration height for the same injection pressure ratio, but $M_\infty h/d_e$ was correlated by equation 4 for both Mach numbers. Changing the injector orifice diameters from A through 6 also resulted in a $M_\infty h/d_e$ which followed equation 4. Therefore, the parameter $M_\infty h/d_e$ for water was found to depend primarily on the ratio of the injection total pressure to the free stream static pressure.

In Fig. 11 the penetration data obtained using injectors A, B, 1, 2, and 6 injecting heptane and the 58 per cent glycerin-42 per cent water mixture are presented and compared to the curve shown in Fig. 10 for water. Within experimental accuracy, the heptane and glycerin-water

mixture followed the penetration curve obtained for water alone. The viscosity of the glycerin-water mixture was 10.9 times greater than water, while the surface tension was approximately the same. This would seem to indicate that for the fluids used in these experiments, surface tension, viscosity, and density did not greatly affect the penetration parameter $M_\infty h/d_e$. It was observed that the data points obtained at Mach 2.8 fell slightly below the reference curve, while 13 of 19 points taken at Mach 4.0 fell above the curve; but no definite conclusions were reached since insufficient additional experiments were performed in that area.

There was no specific indication that the three fluids injected forward into a Mach 2.8 free stream at various angles penetrated further than normal water penetration. It was noted that data scatter with forward injection was less than observed in Fig. 10. No forward injection data were obtained at Mach 4.0. A scattering of approximately ± 10 per cent about the normal water penetration curve in Fig. 12 was considered to be within experimental accuracy. Also, neither viscosity nor surface tension seemed to have any appreciable effect in either increasing or decreasing the penetration parameter $M_\infty h/d_e$, since data were scattered both slightly above and below the reference water curve.

Several photographs of fluids injected forward into the Mach 2.8 cross stream were notable by the absence of a visible shock wave in front of the injected spray near the surface of the plate. This writer concluded that the probable reason for the disappearance of the shock wave was the slightly unsteady nature of the injected fluid flow since the photographs were taken over a relatively long exposure time of 1/125 second when compared to a shadowgraph exposure time of 10^{-7} seconds.

The shadowgraph techniques used in Ref. 16, for example, showed a remarkably close-fitting shock wave system associated with the injection of liquid nitrogen.

Lateral spreading obtained with the side plate model (Fig. 2) is presented in Fig. 13 for heptane, water, and the glycerin-water mixture injection through orifices Double, A, and 2 in Mach 2.8 and 4.0 cross flows. Although data points were limited when compared to the penetration data, sufficient information was considered available to permit inclusion in the study. Figures 30 to 32 are representative photographs used to calculate lateral spreading data points.

Mach 2.8 lateral spreading data were obtained for a relatively small injection pressure ratio range of 160 to 360. The Mach 4.0 injection pressure ratios ranged from 25 to 825. Spreading data were limited by (1) free stream stagnation pressures available and (2) injection total pressures within a range of 30 to 1500 psia. which would not splatter the observation window with injectant. Increasing the free stream stagnation pressure permitted higher injectant total pressures to be utilized.

The Mach 4.0 data do, nevertheless, approximate a straight line function when plotted on a log-log scale and are represented by

$$\frac{W}{d_e} = 18.9 \left(\frac{P_{oj}}{P_1}\right)^{0.197} . \qquad (6)$$

Also plotted on Fig. 13 is the equation obtained for lateral spreading at Mach 2.8 in Ref. 38, which is

$$\frac{W}{d_e} = 27.0 \left(\frac{P_{oj}}{P_1}\right)^{0.133} . \qquad (7)$$

It should be noted that the Mach 2.8 spreading data obtained in this study, which are somewhat lower that either equation 6 or 7, were not included in the data for equation 6.

Tests on floodlight location and intensity performed during this study and later by Ref. 43 indicated a variation in the spray pattern dimensions when one or both conditions were changed. Reducing the intensity by filtering noticeably reduced the spray dimensions in the lateral spreading photographs by 20 to 25 per cent in Ref. 43. A tendency for the intensity of the movie flood lamps to decrease with hours in operation was not detected until well into the experimental program. Fortunately, data for each Mach number were obtained using relatively short floodlamp operating times; therefore, each set of data remained consistent. Since additional experiments performed in Ref. 43 indicated agreement of the Mach 2.8 and 4.0 lateral spreading data using an electronic flash lighting system, it was reasonably assumed that lighting conditions could have produced a 20 per cent reduction in the Mach 2.8 lateral spreading obtained by this study.

Lateral spreading was therefore determined to be a primary function of orifice diameter and a lesser function of the injection pressure ratio. The injectant fluid properties did not make any appreciable change in the spreading parameter. Since the Mach 2.8 data reported in this thesis are 20 per cent lower due to lighting conditions discussed previously, lateral spreading can be considered Mach number independent.

An effort was made to obtain additional information on the flow field in front of the injected fluid jet. Composite schlieren and scattered light photographs in Figs. 14 to 21 were used for this purpose. The photographs show extraneous details which are noted below.

The Mach lines in the upper left corner were caused by an intersection of the tunnel wall and an observation window. A chipped outside face of one window photographed as a white spot in the center of the photographs, and the Mach lines emanating from the leading edge of the flat plate were due to slight irregularities in the leading edge. Ice formation observed on the after section of the plate on several photographs was caused by the low free stream static temperatures. Static pressure readings taken ahead and aft of the plate leading edge Mach lines indicated no measurable pressure differences, thereby indicating a very weak disturbance at the leading edge.

An inspection of Figs. 16-20 indicated curvature of the bow shock wave in front of the liquid jet from the surface of the plate for a distance of several orifice diameters along the jet. This curvature could be due to one or both of the following effects: One, a stagnation point occurred on the surface of the plate in front of the orifice during fluid injection. The resulting adverse pressure gradient caused separation of the boundary layer and a detached shock wave system was formed. Two, additional curvature of the shock may be due to distortion of the liquid jet by the supersonic cross flow. Clark in Ref. 35 proposed a model for the liquid jet breakup in a cross flow of gas which consisted of a liquid jet progressively spreading transverse to the free stream in response to the pressure distribution at the liquid jet surface and resisted primarily by the inertia of the liquid. Since the liquid jet was initially a small diameter cylindrical cross section, transverse spreading of the liquid jet distorted the cross section and presented a larger frontal area to the cross flow. The standoff distance would therefore increase as the bow shock wave approached a normal shock in front of the distorted jet cross section. Thus the

first effect would form the base of the bow shock wave system, and the second effect would gradually increase the standoff distance. Both effects were considered effective for only a short distance above the plate surface in the region where the liquid jet was approximately a solid cylindrical body, since the momentum of the cross stream rapidly turned the liquid jet downstream and increased the curvature of the bow shock wave.

In Fig. 19 the detached shock wave of a liquid jet injected forward into a Mach 2.8 cross stream was notably stronger than those observed for normal injection. It was considered that the increased strength of the bow shock wave could be a factor in observing no significant increase in the penetration parameter $M_\infty h/d_e$ due to forward injection, although an increase was observed in Ref. 11.

The flow fields around a solid cylindrical rod and a liquid jet injected through a circular orifice when placed in a supersonic cross flow were investigated to determine the possibility of obtaining a correlation between the two fields. D. M. Sykes studied the supersonic and low speed flow past circular cylinders of finite length supported at one end in Ref. 44. Sykes divided the cylinder into three areas of study -- the free end, the center section, and the supported end -- and suggested that cylinders must have a length-to-diameter ratio of four to avoid any interaction of effects between the free and the supported ends of the cylinder.

In Fig. 21 a 0.125 inch diameter solid cylinder is shown placed normal to a Mach 2.8 cross flow, with essentially the same free stream static and total pressures as those of Fig. 20, where water was injected normal to a Mach 2.8 cross flow. It was evident that the free end flow fields were not similar, since the expected breakup and spreading of

the injected fluid jet influenced the shape of the bow shock wave in Fig. 20. A close inspection of the center and supported sections of the rod in Fig. 21 with the lower portion of the fluid jet in Fig. 20 indicates similarities in the separation and bow shock wave shapes. It was observed that shock waves associated with the flow field around the solid body were generally stronger than those for a similar sized injected fluid jet. Insufficient observations were made to determine whether or not a smaller diameter solid rod would provide a proper correlation between the rod and a fluid jet. Measurement of the pressure field on the surface aft of the rod and the injected jet would provide a direct correlation between the two flow fields. Additional information in this area could provide a method of correlating the flow fields around solid cylindrical rods and an injected fluid jet, eliminating the requirements for physically injecting the fluids and providing a more simplified technique for predicting the pressure distribution around an injected fluid jet due to the external flow field.

There was evidence to indicate that the higher viscosity fluids injected through the larger orifices tend to have a significant effect on separation and the associated shock system. The penetration photograph in Fig. 22 shows the glycerin-water mixture injected through a 0.050 inch diameter orifice into a Mach 2.8 cross stream where the injection pressure ratio was 234. A very strong separation shock was formed ahead of the injector, and injectant fluid was observed in the separated region. Undoubtedly the wedge of injectant fluid upstream caused the oblique separation shock wave. In Fig. 23 the only changes to the previous conditions were injection through injector 2 (0.040 inch diameter) at a lower (186) injection pressure ratio. Although the separation shock ahead of the injector was also visible in this

photograph, there was no evidence of an adverse pressure gradient strong enough to cause injectant fluid to flow forward into the separated region.

The effects of the injectant physical properties were not observed to affect the penetration parameter significantly, but Figs. 24 through 26 indicated that an additional consideration of the concentration or "core" of the injectant jet may also be important. An examination of these photographs showed that the lower surface tension fluid heptane shown in Fig. 25 breaks up more rapidly into smaller droplets than either water (Fig. 24) or the glycerin-water mixture (Fig. 26). Therefore the core of a fluid which had a relatively low surface tension such as heptane may be more evenly dispersed over a larger volume. This effect could be of significant importance in re-entry vehicle communications when considering use of an electronegative species injected into the plasma sheath. Since the electron density is not uniform throughout the plasma layer, a low surface tension fluid injection could reduce the electron density significantly if the penetration were properly correlated to the electron density variation and the plasma layer thickness.

An attempt was made to determine the location of the "core" of the injectant spray. Figures 27, 28, and 29 are flow visualization photographs of water injection through injector X at exposure times of 1/125, 1/250, and 1/500 seconds respectively. The liquid jet was observed to remain essentially collimated for 7 to 8 diameters above the plate surface and then to spread gradually from that point until it was approximately one-half the maximum penetration height. At that point the momentum of the free stream had reduced the liquid jet momentum and started the rapid curvature of the jet downstream. Measurements from

Fig. 29 showed that the centerline of the core became parallel to the plate surface before the maximum penetration height was reached. Also, the centerline was located at approximately 65-70 per cent of the maximum penetration height. This supports the suggestion that the liquid jet tended to remain well collimated when injected at high injectant total pressures. It appeared that although distortion of the jet starts within a few diameters of the surface, as evidenced by the shape of the bow shock wave, jet breakup was limited until the jet turned downstream.

VI. CONCLUSIONS

Penetration of a liquid jet of heptane, water, or 58 per cent glycerin-42 per cent water (by mass) injected normal to Mach 2.8 and 4.0 cross streams, when properly non-dimensionalized, can be represented as a function of the injection pressure ratio only. The penetration parameter was not noticeably affected by a variation of the fluid properties of surface tension, viscosity, or density, or by changes in the Mach number or free stream total pressure. Within experimental accuracy, the variation of orifice diameters and injector length-to-diameter ratios did not change the penetration parameter. Forward liquid injection was not observed to significantly affect the penetration parameter.

Lateral spreading was determined to be a primary function of orifice diameter and a secondary function of the injection pressure ratio. Neither the injectant fluid properties nor the orifice diameter and the injector length-to-diameter ratios were observed to make any appreciable change in the spreading parameter. Lateral spreading was also insensitive to Mach number variation.

REFERENCES

1. Dix, D. M., Golden, K. E., Taylor, E. C., Kolpin, M. A., and Caron, P. R., Lifting Re-entry Communications, TR-669(6220-10)-3, Vol. 1, Aerospace Corporation (May 1966).

2. Good, R. E., and Rossi, J. J., An Injection System for Alleviation of Radio Blackout During Re-entry, MC 63-78-R2, Mithras, Inc. (Jan. 1966).

3. Cuddihy, W. F., Beckwith, I. E., and Schroeder, L. C., "A Solution to the Problem of Communications Blackout of Hypersonic Re-entry Vehicles," AMRAC Proceedings, IX (II), 187-231 (1963).

4. Cuddihy, W. F., and Hughes, J. K., Simulated Re-entry Tests of a Method for Reducing Radio Blackout by Material Addition to Ionized Flow Fields, TMX-988, NASA (Aug. 1964).

5. Cuddihy, W. F., Beckwith, I. E., and Schroeder, L. C., RAM B2 Flight Test of a Method for Reducing Radio Attenuation During Hypersonic Re-entry, TMX-902, NASA (Oct. 1963).

6. Beckwith, I. E., and Huffman, J. K., Injection and Distribution of Liquids in the Flow Fields of Blunt Shapes at Hypersonic Speeds, TMX-989, NASA (Aug. 1964).

7. Ferri, A., Libby, P. A., and Zakkay, V., Theoretical and Experimental Investigation of Supersonic Combustion, PIBAL Report No. 713, Polytechnic Institute of Brooklyn (Sept. 1962) 119 pp.

8. Ferri, A., Moretti, G., and Slutsky, S., "Mixing Processes in Supersonic Combustion," Paper presented at Meeting of Society for Industrial and Applied Mathematics, Washington, D. C., May 11-14, 1964.

9. Ferri, A., "Review of Problems in Application of Supersonic Combustion," 7th Lanchester Memorial Lecture, RAS, London, England, May 14, 1964. Journal of the Royal Aeronautical Society, Vol. 68, No. 645 (Sept. 1964), pp. 575-595.

10. Ferri, A., "Supersonic Combustion Progress," Astronautics and Aeronautics, Part I, Vol. 2, No. 8 (Aug. 1964), pp. 32-37.

11. Forde, J. M., Molder, S., and Szpiro, E. J., "Secondary Liquid Injection into a Supersonic Airstream," J. Spacecraft and Rockets, Vol. 3, No. 8 (Aug. 1966), pp. 1172-1176.

12. Green, C. J., and McCullough, Foy, Jr., "Liquid Injection Thrust Vector Control," AIAA Journal, Vol. 1, No. 3 (March 1963), pp. 573-578.

13. Hsia, H. T-S., Seifert, H. S., and Karamcheti, K., "Shocks Induced by Secondary Fluid Injection," J. Spacecraft and Rockets, Vol. 2, No. 1 (Jan.-Feb. 1965), pp. 67-72.

14. Hsia, H. T-S., "Equivalence of Secondary Injection to a Blunt Body in Supersonic Flow," AIAA Journal, Vol. 4, No. 10 (Oct. 1966), pp. 1832-1834.

15. Schgal, R., and Wu, J. M., A Study of Thrust Vector Control by Liquid Injection into a Rocket Nozzle, TM No. 33-138, Jet Propulsion Laboratory (May 1963).

16. Dowdy, M. W., and Newton, J. F., Jr., Investigation of Liquid and Gaseous Secondary Injection Phenomena on a Flat Plate with M=2.01 to M=4.54, TP No. 32-542, Jet Propulsion Laboratory (Dec. 1963).

17. Walker, R. E., Stone, A. P., and Shandor, M., Secondary Gas Injection in a Conical Rocket Nozzle, 1: Effect of Orifice Diameter and Molecular Weight of Injectant, Johns Hopkins University, Applied Physics Laboratory Report CM-1010 (Feb. 1962).

18. Schetz, J. A., and Billig, F. S., "Penetration of Gaseous Jets Injected into a Supersonic Stream," J. Spacecraft and Rockets, Vol. 3, No. 11 (Nov. 1966), pp. 1658-1665.

19. Broadwell, J. E., An Analysis of the Fluid Mechanics of Secondary Injection for Thrust Vector Control, Space Technology Labs. Report 6120-7744-MU-000 (March 1962).

20. Zukoski, E. E., and Spaid, F. W., "Secondary Injection of Gases into a Supersonic Flow," AIAA Journal, Vol. 2, No. 10 (Oct. 1964), pp. 1689-1696.

21. Spaid, F. W., and Zukoski, E. E., "Further Experiments Concerning Secondary Injection of Gases into a Supersonic Flow," AIAA Journal, Vol. 4, No. 12, (Dec. 1966), pp. 2216-2218.

22. Sterrett, J. R., Barber, J. B., Alston, D. W., and Romeo, D. J., Experimental Investigation of Secondary Jets from Two-dimensional Nozzles with Various Exit Mach Numbers for Hypersonic Control Application, NASA Tech. Note, TN D-3795 (Jan. 1967).

23. McRae, R. P., Experimental Investigations of a Liquid Jet Injected into a Mach 4 Stream, Douglas Aircraft Co., Santa Monica, Calif., Report SM-47879 (May 1966).

24. Billig, F. S., A Study of Combustion in Supersonic Streams, Johns Hopkins University, Bumblebee Report 321 (July 1964).

25. Karamcheti, K., and Hsia, H. T-S., "Integral Approach to an Approximate Analysis of Thrust Vector Control by Secondary Injection," AIAA Journal, Vol. 1, No. 11 (Nov. 1963), pp. 2538-2544.

26. Broadwell, J. E., "An Analysis of the Fluid Mechanics of Secondary Injection for Thrust Vector Control," AIAA Journal, Vol. 1, No. 5 (May 1963), pp. 1067-1075.

27. Ferrari, C., Interference Between a Jet Issuing Laterally from a Body and the Enveloping Supersonic Stream, Johns Hopkins University, Bumblebee Report 286, April 1959.

28. Green, C. J., and Benham, C. B., Parameters Controlling the Performance of Secondary Injection, U. S. Naval Ordnance Test Station, China Lake, Calif., NAVWEPS 7743, NOTS 2710 (Dec. 1961).

29. Charwat, A. F., and Allegre, J., "Interaction of a Supersonic Stream and a Transverse Supersonic Jet," AIAA Journal, Vol. 2, No. 11 (Nov. 1964), pp. 1965-1972.

30. Orth, R. C., and Funk, J. A., "An Experimental and Comparative Study of Jet Penetration in Supersonic Flow," AIAA Paper No. 67-225 presented at the Fifth Aerospace Sciences Meeting, New York, Jan. 23-26, 1967.

31. Schetz, J. A., Hawkins, P. F., and Lehman, H., "Structure of Highly Underexpanded Transverse Jets in a Supersonic Stream," AIAA Journal, Vol. 5, No. 5 (May 1967), pp. 882-884.

32. Adelberg, M., "Breakup Rate and Penetration of a Liquid Jet in a Gas Stream," AIAA Journal, Vol. 5, No. 8 (Aug. 1967), pp. 1408-1415.

33. Wu, J. M., Chapkis, R. L., and Mager, A., "Approximate Analysis of Thrust Vector Control by Fluid Injection," ARS Journal, Vol. 31, No. 12 (Dec. 1961), pp. 1677-1685.

34. Fuhs, A. E., Spray Formation and Breakup and Spray Combustion, AMB/TD No. 1199, Tech. Note No. 4, Sundstrand Turbo. (Feb. 1958).

35. Clark, B. J., Breakup of a Liquid Jet in a Transverse Flow of Gas, NASA TN D-2424 (Aug. 1964).

36. Schmidt, J. M., An Experimental Study of the Behavior of Liquid Streams Injected into a Low-Pressure Chamber, Progress Report No. 4-94, Jet Propulsion Laboratory (April 1949).

37. Lee, D. W., Experiments on the Distribution of Fuel in Fuel Sprays, NACA Report No. 438 (Feb. 1932).

38. Kolpin, M. A., Horn, K. P., and Reichenbach, R. E., "A Study of Penetration of a Liquid Injectant into a Supersonic Flow," AIAA Journal (in press).

39. Lewis, H. C., Edwards, D. G., Goglia, M. J., Rice, R. I., and Smith, L. W., "Atomization of Liquids in High Velocity Gas Streams," Ind. and Engrg. Chem., Vol. 40, No. 1 (Jan. 1948), pp. 67-74.

40. Putnam, A. A., et al., Injection and Combustion of Liquid Fuels, WADC Tech. Report 56-344, Battelle Memorial Institute (March 1957).

41. Harmon, D. B., McRae, R. P., and Parker, B. J., Final Report-Cold Flow Experimental Studies of the Breakup of Non-Reactive Liquid Jets Injected into a Supersonic Cross Flow, Douglas Report SM-48213 (Confidential), Douglas Aircraft Company, Santa Monica, Calif. (April 1966).

42. Weast, R. C. (ed.), Handbook of Physics and Chemistry, 45th ed., The Chemical Rubber Co., Cleveland, 1964.

43. Reichenbach, P. E., and Horn, F. P., personal communication (Nov. 1967).

44. Sykes, D. M., "The Supersonic and Low-speed Flows Past Circular Cylinders of Finite Length Supported at One End," Journal of Fluid Mechanics, Vol. 12, Part 3 (March 1962), pp. 367-387.

TABLE I

INJECTOR CHARACTERISTICS

Injector (Note 1)	d_o (in.)	d_e (in.)	θ^* (deg.)	L/d_o	L/d_e	Symbols Water M2.8	Water M4.0	Glycerin M2.8	Glycerin M4.0	Heptane M2.8	Heptane M4.0
A	.0210	.0178	0		2.5						
B	.0145	.0117	0		4.0						
X	.0210	.0170	+5		2.3						
Double	(2).0145	.0163	0		5.3						
1	.0520	.0439	0	3.2	3.6						
2	.0420	.0335	0	3.6	4.3						
3	.0430	.0335	+20	3.3	4.0						
4	.0410	.0335	+30	3.4	4.0						
5	.0420	.0335	+45								
6	.8010	.0624	0								

* +Indicates θ is measured positive in the forward direction

Note 1. Injectors A, B, X, and Double courtesy Aerospace Corporation.

Note 2. M2.8, M4.0 denote Mach numbers 2.8 and 4.0 respectively.

TABLE II

LIQUID INJECTANT PROPERTIES

Fluid	Surface Tension (lb/sec)	Density (lb/cu.ft.)	Viscosity [lb/(ft-sec)]
Water	0.161	62.4	6.72×10^{-4}
Heptane	0.045	42.6	2.75×10^{-4}
58% Glycerin-42% water mixture (by mass)	0.150	71.4	6.15×10^{-3}

Note 1. Fluid properties at 530 °R.

TABLE III-1

SUMMARY OF DATA AND CALCULATED VALUES

MACH = 2.8

Run	Fluid	Injector	P_{o_t} (psia)	P_{o_j} (psia)	P_1 (psia)	T_1 (°R.)	P_{o_j}/P_1	Calculations			
								Observed		Extrapolated	
								$1/d_e$	$\frac{M_2 h}{d_e}$	$1/d_e$	$\frac{M_2 h}{d_e}$
1-1	Water	2	87.0	380	2.86	206	133	75	100	150	111
1-2	"	2	80.2	750	2.94	"	255	75	120	150	138
1-3	"	2	114.0	750	4.18	"	179	75	108	150	124
1-4	"	2	114.7	750	4.21	"	178	75	111	150	127
1-5	"	2	80.6	400	2.96	"	135	75	91	150	105
1-6	"	2	80.0	1100	2.96	"	372	75	148	150	170
1-7	"	2	119.3	1570	4.32	"	363	75	148	150	171
1-8	"	3	80.5	420	2.93	"	143	75	123	150	141
1-9	"	3	81.0	800	2.93	"	273	75	145	150	160
1-10	"	3	81.0	1200	2.97	"	404	75	149	150	164
1-11	"	3	80.9	770	2.96	"	260	75	138	150	153
1-12	"	3	121.0	780	4.45	"	175	75	102	150	112
1-13	"	3	118.9	1190	4.35	"	274	75	131	150	144

TABLE III-2

SUMMARY OF DATA AND CALCULATED VALUES

MACH = 2.8

Run	Fluid	Injector	P_{ot} (psia)	P_{oj} (psia)	P_1 (psia)	T_1 (°R.)	P_{oj}/P_1	Calculations			
								Observed		Extrapolated	
								$1/d_e$	$\frac{X_s h}{d_e}$	$1/d_e$	$\frac{X_s h}{d_e}$
1-14	Water	3	120.4	1560	4.41	206	354	75	154	150	169
1-17	"	4	80.8	780	2.96	"	138	75	108	150	119
1-21	"	4	47.8	215	1.76	"	122	75	105	150	120
1-23	"	4	60.1	400	2.18	"	183	75	102	150	112
1-24	"	A	118.0	800	4.20	"	190	150	132		
1-25	"	A	118.9	1990	4.35	"	457	150	177		
1-26	"	A	120.8	2050	4.38	"	468	150	192		
1-27	"	A	121.8	2960	4.45	"	665	150	168		
1-28	"	X	61.8	1050	2.24	"	468	150	188		
1-29	"	X	120.5	2010	4.40	"	456	150	185		
1-30	"	X	119.0	2950	4.35	"	678	150	227		
1-31	"	X	61.7	1520	2.24	"	678	150	223		
1-32	"	X	61.7	1530	2.24	"	683	150	218		

TABLE III-3

SUMMARY OF DATA AND CALCULATED VALUES

MACH = 2.8

Run	Fluid	Injector	P_{ot} (psia)	P_{oj} (psia)	P_1 (psia)	T_1 (°R.)	P_{oj}/P_1	Calculations			
								Observed		Extrapolated	
								$1/d_e$	$\frac{M_\infty h}{d_e}$	$1/d_e$	$\frac{M_\infty h}{d_e}$
1-33	Water	X	61.7	1530	2.24	206	683	150			
1-34	"	X	61.8	1500	2.25	"	666	150			
1-35	"	X	61.7	1500	2.24	"	669	150			
1-37	Glycerin	X	119.0	1010	4.36	"	231	150	153		
1-38	"	X	119.0	1970	4.36	"	451	150	180		
1-39	"	X	80.8	2950	2.93	"	1006	150	245		
1-40	"	2	117.9	810	4.34	"	186	75	102	150	112
1-41	"	2	119.0	1550	4.35	"	356	75	123	150	135
1-42	"	3	81.8	1000	2.95	"	338	75	127	150	140
1-44	"	1	118.9	1020	4.35	"	234	75	80	150	88
1-45	Water	1	61.4	800	2.20	"	363	75	106	150	117
1-47	Glycerin	Double	81.4	2000	2.94	"	680	150	196		
1-48	Water	Double	81.0	2040	2.91	"	701	150	196		

TABLE III-4

SUMMARY OF DATA AND CALCULATED VALUES

MACH = 2.8

Run	Fluid	Injector	P_{ot} (psia)	P_{oj} (psia)	P_1 (psia)	T_1 (°R.)	P_{oj}/P_1	Calculations			
								Observed		Extrapolated	
								$1/d_e$	$\frac{M_e h}{d_e}$	$1/d_e$	$\frac{M_e h}{d_e}$
1-49	Heptane	Double	80.6	2060	2.89	206	713	150	205		
1-50	"	X	81.3	1950	2.92	"	667	150	190		
1-51	"	X	119.0	1980	4.35	"	455	150	159		
1-53	"	2	81.0	1000	2.90	"	344	75	127	150	140
1-54	"	4	80.6	1040	2.88	"	361	75	136	150	156
1-55	"	4	80.6	980	2.88	"	340	75	138	150	158

TABLE III-5

SUMMARY OF DATA AND CALCULATED VALUES

MACH = 2.8

Run	Fluid	Injector	P_{ot} (psia)	P_{oj} (psia)	P_1 (psia)	T_1 (°R.)	P_{oj}/P_1	Calculations			
								Observed		Extrapolated	
								$1/d_e$	$\frac{W}{d_e}$	$1/d_e$	$\frac{W}{d_e}$
1-57	Glycerin	2	80.9	790	2.95	206	268	75	46.17		
1-60	Water	Double	81.1	1000	2.96	"	338	150	51.0		
1-63	"	Double	119.8	1590	4.40	"	361	150	49.4		
1-64	Glycerin	Double	120.0	1540	4.41	"	349	150	51.0		
1-65	Heptane	Double	119.8	970	4.40	"	20	150	40.8		
1-70	Water	A	81.5	500	2.95	"	169	150	42.1		
1-71	Glycerin	A	80.6	500	2.94	"	170	150	43.7		
1-72	Glycerin	A	80.6	500	2.94	"	170	150	40.8		
1-73	Heptane	A	80.9	480	2.95	"	163	150	40.5		

Note 1. Runs 1-1 through 1-55 are normal and forward penetration data.

Runs 1-57 through 1-73 are spreading data.

TABLE IV-1

SUMMARY OF DATA AND CALCULATED VALUES

MACH = 4.0

Run	Fluid	Injector	P_{ot} (psia)	P_{oj} (psia)	P_1 (psia)	T_1 (°R.)	P_{oj}/P_1	Calculations			
								Observed		Extrapolated	
								$1/d_e$	$\frac{M_e h}{d_e}$	$1/d_e$	$\frac{M_e h}{d_e}$
2-1	Water	A	144.5	940	0.95	126	1031	150	302		
2-3	Heptane	A	144.2	990	.94	"	1053	150	267		
2-4	Glycerin	A	144.2	1000	.93	"	1064	150	293		
2-5	"	A	144.3	1000	.93	"	1064	150	315		
2-6	"	1	149.4	180	1.01	"	179	75	71	150	80
2-7	"	1	164.0	195	1.09	"	179	50	105	150	118
2-8	Water	1	164.0	195	1.09	"	179	50	113	150	121
2-9	Heptane	1	144.2	200	0.94	"	213	50	125	150	148
2-10	Water	1	144.0	200	0.94	"	214	75	133	150	148
2-11	"	1	144.0	200	0.94	"	214	75	123	150	142
2-12	"	B	144.0	2980	0.94	"	3187	150	428		
2-13	"	B	144.0	2980	0.94	"	3187	150	449		
2-14	Glycerin	B	144.5	2800	0.94	"	2974	150	417		

TABLE IV-2

SUMMARY OF DATA AND CALCULATED VALUES

MACH = 4.0

Run	Fluid	Injector	P_{ot} (psia)	P_{oj} (psia)	P_1 (psia)	T_1 (°R.)	P_{oj}/P_1	Calculations			
								Observed		Extrapolated	
								$1/d_e$	$\frac{M_\infty h}{d_e}$	$1/d_e$	$\frac{M_\infty h}{d_e}$
2-15	Heptane	B	144.5	2770	0.94	126	2947	150	459		
2-17	Water	6	143.3	101	0.93	"	109	50	84	150	100
2-18	"	6	151.0	49	0.99	"	50	50	68	150	80
2-19	"	6	151.0	52	0.99	"	52	50	59	150	69
2-20	"	6	151.0	50	0.99	"	52	50	68	150	80
2-21	"	6	151.0	47	0.99	"	48	50	65	150	75
2-22	"	6	151.8	47	0.99	"	47	50	55	150	64
2-23	"	6	151.0	50	0.99	"	50	50	55	150	64
2-24	Heptane	6	151.0	51	0.99	"	51	50	76	150	89
2-25	Glycerin	6	151.8	50	1.00	"	50	50	61	150	74
2-27	"	6	149.7	53	0.98	"	54	50	67	150	78
2-28	Water	6	144.5	54	0.94	"	57	50	76	150	90
2-42	"	6	149.5	39	0.97	"	41	50	56	150	65

TABLE IV-3

SUMMARY OF DATA AND CALCULATED VALUES

MACH = 4.0

Run	Fluid	Injector	P_{ot} (psia)	P_{oi} (psia)	P_1 (psia)	T_1 (°R.)	P_{oi}/P_1	Calculations			
								Observed		Extrapolated	
								l/d_e	$\frac{M_{ph}}{d_e}$	l/d_e	$\frac{M_{ph}}{d_e}$
2-43	Water	6	147.5	15	0.95	126	16	5	57	150	66
2-45	"	6	147.5	30	0.95	"	33	50	68	150	79
2-46	"	6	151.9	29	0.99	"	29.4				
2-47	Heptane	2	144.7	30	0.93	"	32	75	70	150	86
2-48	"	2	144.5	30	0.94	"	31	75	81	150	92
2-49	"	2	151.8	51	1.00	"	51	75	60	150	88
2-50	"	2	151.8	20	1.00	"	20			150	74
2-53	Water	2	174.5	75	1.17	"	64			150	98
2-55	"	2	143.2	30	0.92	"	33			150	86
2-56	"	2	143.3	32	0.93	"	34			150	72
2-58	"	2	144.3	39	0.94	"	41			150	95
2-60	"	2	144.5	30	0.94	"	32			150	81

TABLE IV-4

SUMMARY OF DATA AND CALCULATED VALUES

MACH = 4.0

Run	Fluid	Injector	P_{ot} (psia)	P_{oj} (psia)	P_1 (psia)	T_1 (°R.)	P_{oj}/P_1	Calculations			
								Observed		Extrapolated	
								$1/d_e$	$\frac{M_\infty h}{d_e}$	$1/d_e$	$\frac{M_\infty h}{d_e}$
2-61	Water	2	147.0	50	0.96	126	52			150	100
2-62	"	2	145.8	75	0.94	"	80			150	110
2-63	Heptane	2	156.3	75	1.03	"	73			150	78
2-64	"	2	161.3	200	1.07	"	187			150	120
2-65	"	2	156.3	150	1.03	"	145			150	117
2-66	"	2	147.0	200	0.96	"	208			150	142
2-67	Water	6	144.7	90	0.93	"	97			150	90
2-69	"	6	149.6	90	0.97	"	93			150	67

TABLE IV-5

SUMMARY OF DATA AND CALCULATED VALUES

MACH = 4.0

Run	Fluid	Injector	P_{ot} (psia)	P_{oj} (psia)	P_1 (psia)	T_1 (°R.)	P_{oj}/P_1	Calculations Observed $1/d_e$	Calculations Observed $\frac{Y}{d_e}$
2-35	Water	2	187.2	30	1.19	126	25	150	27
2-36	Water	2	151.8	98	1.00	"	98	150	51
2-37	Water	2	159.1	200	1.05	"	190	150	49
2-38	Heptane	2	187.2	150	1.25	"	120	150	46
2-39	Glycerin	2	151.0	150	0.98	"	152	150	58
2-41	Glycerin	2	149.4	150	1.01	"	148	150	53
2-70	Glycerin	2	149.4	640	1.21	"	530	150	70
2-71	Glycerin	2	149.4	315	1.21	"	260	150	59
2-72	Glycerin	A	149.4	1010	1.19	"	850	150	79

Note 1. Runs 2-1 through 2-34 and 2-48 through 2-69 are normal and forward injection penetration data.

2. Runs 2-35 through 2-41 and 2-70 through 2-72 are lateral spreading data.

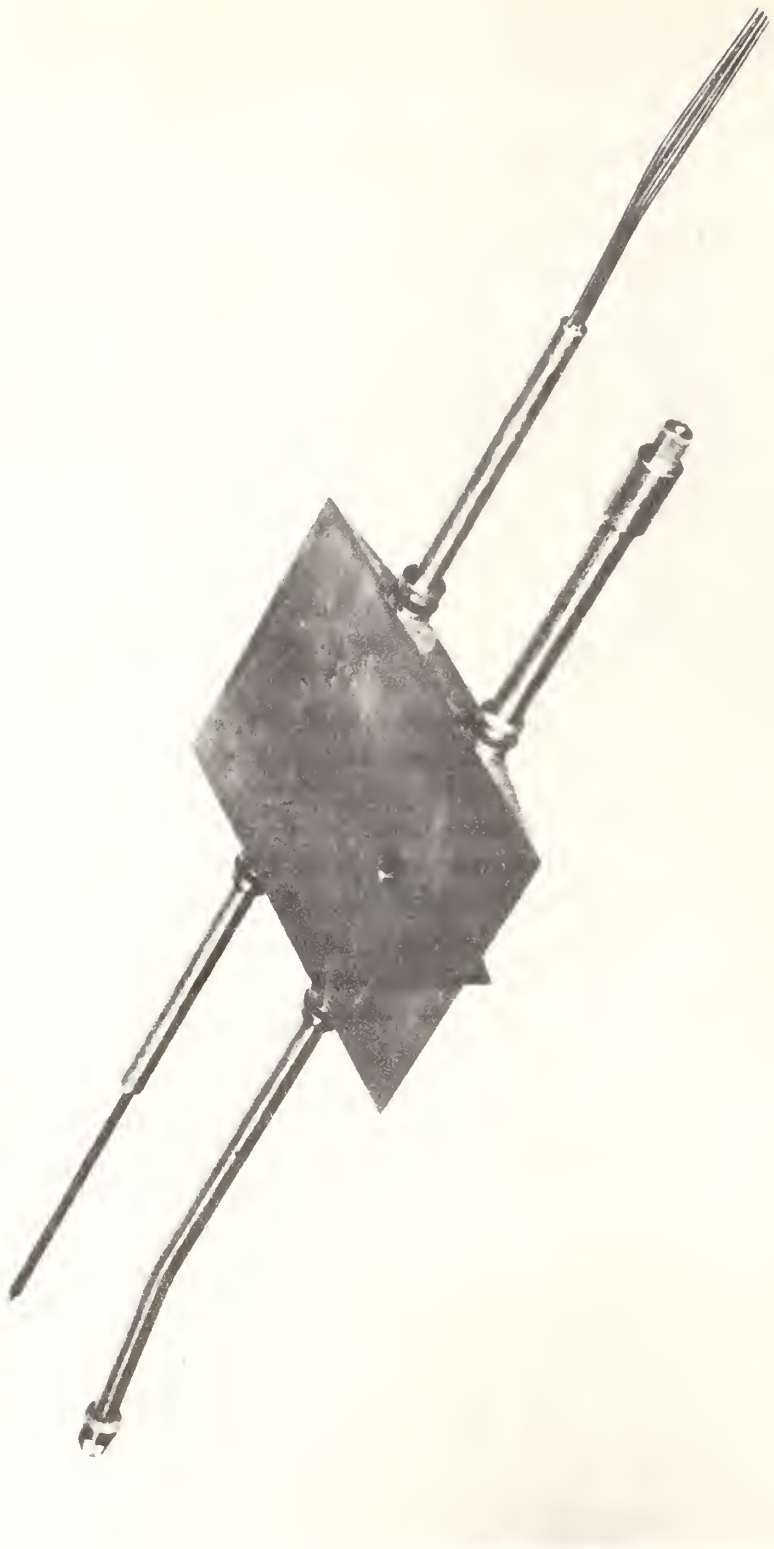


Fig. 1 Flat plate model used to obtain penetration data

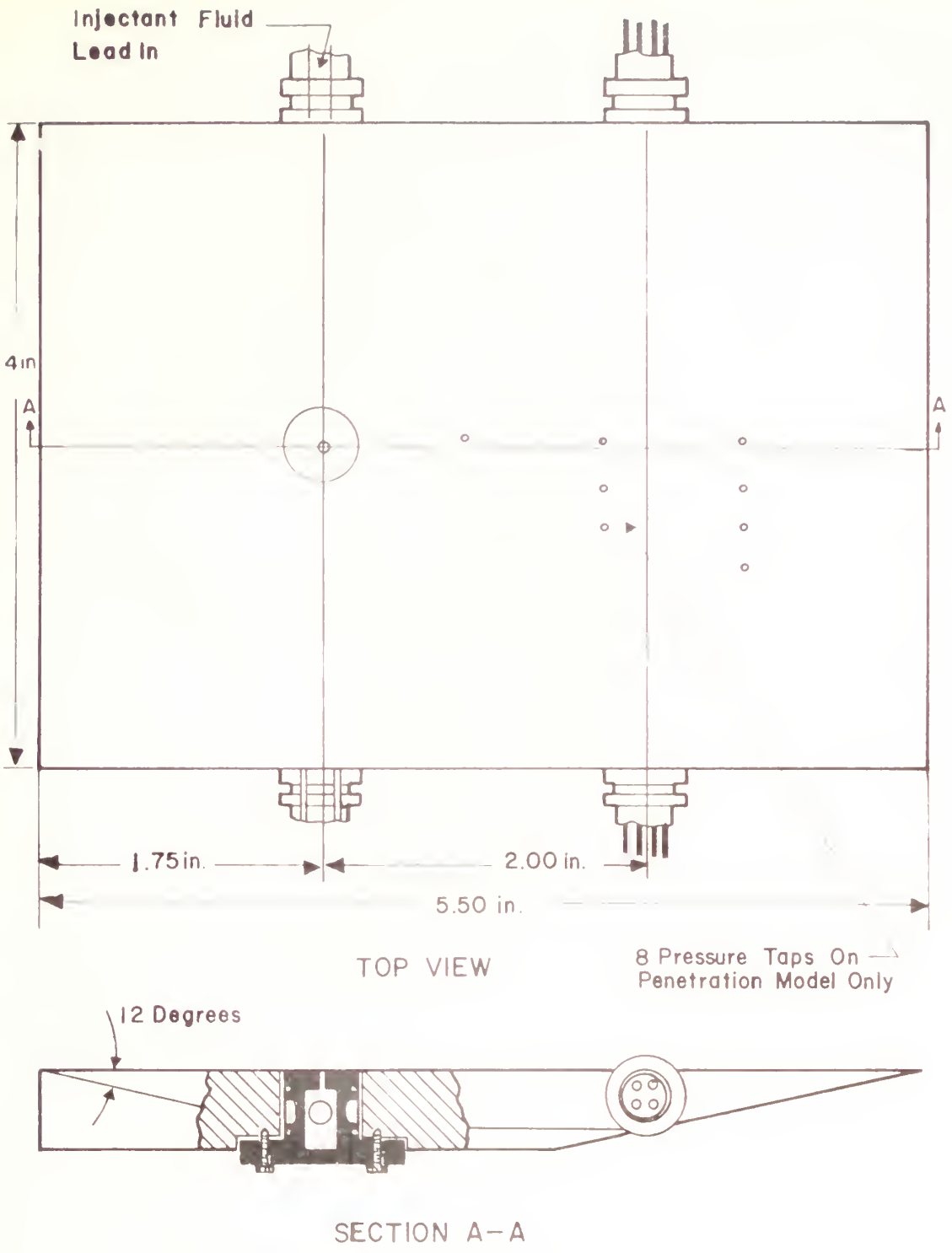


FIG. 2 LAYOUT OF THE FLAT PLATE MODEL USED TO OBTAIN PENETRATION DATA

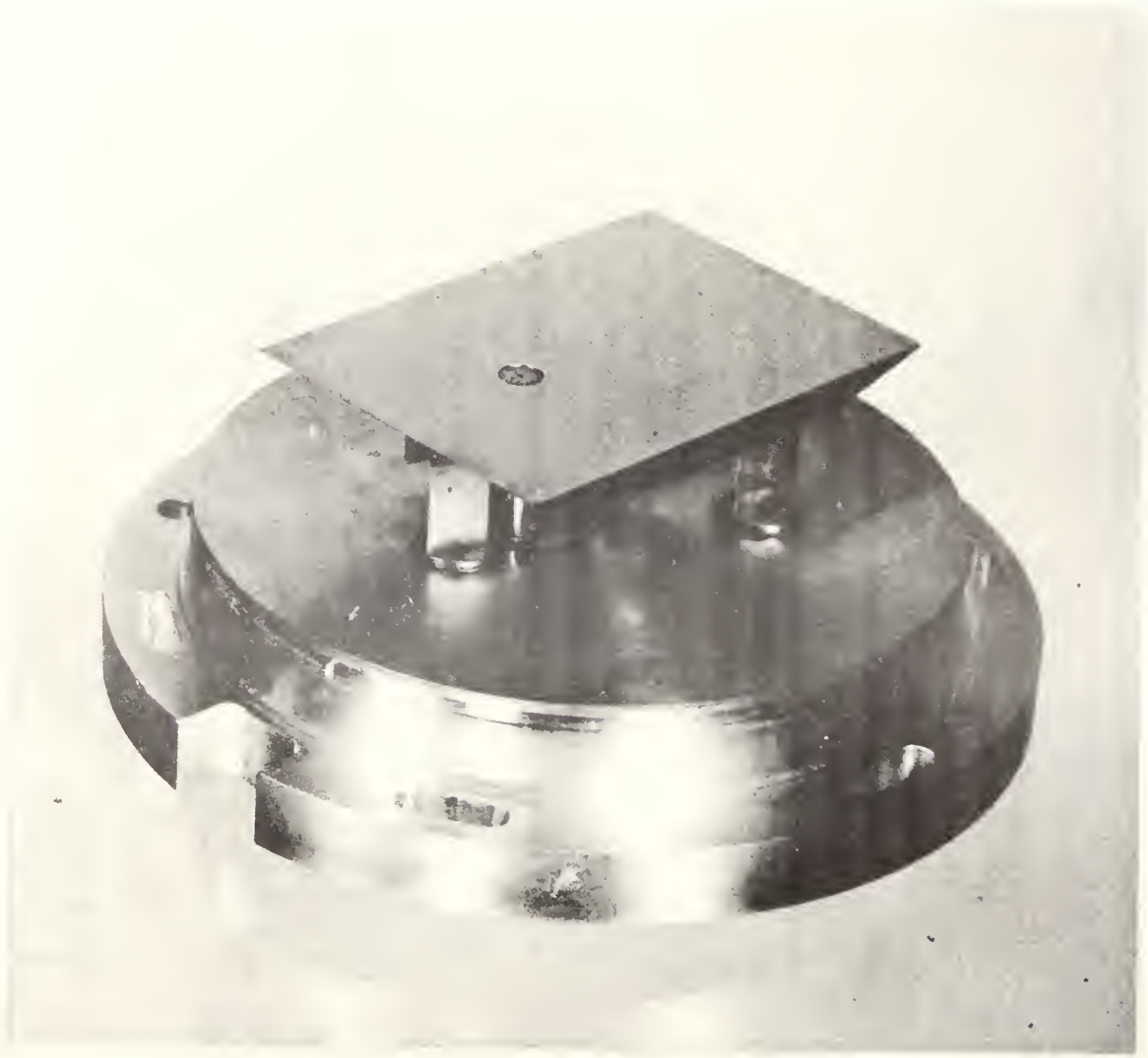


Fig. 3 Flat plate model used to obtain lateral spreading data

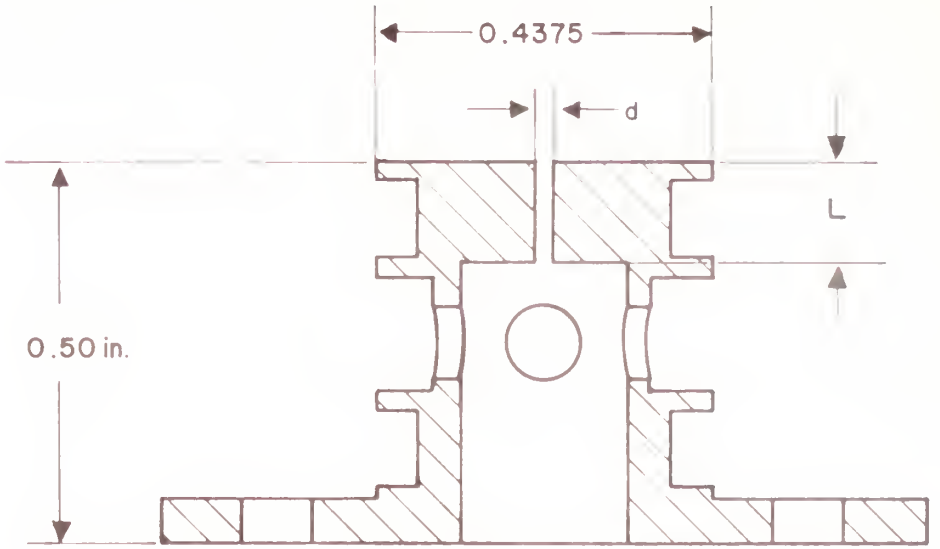


FIG. 4 CROSS SECTION OF AN INJECTOR

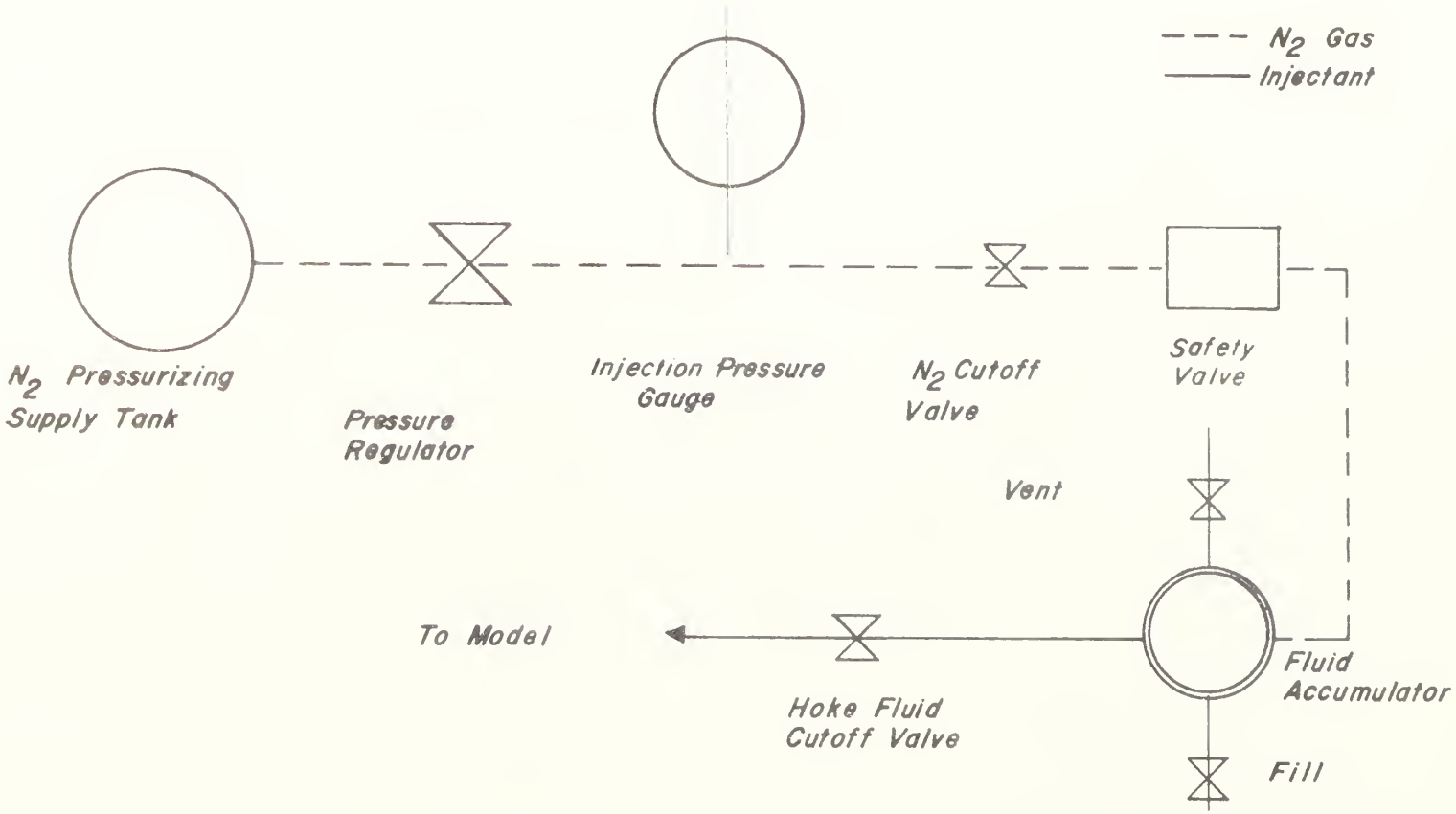


FIG. 5 SCHEMATIC DIAGRAM OF THE LIQUID INJECTOR SYSTEM

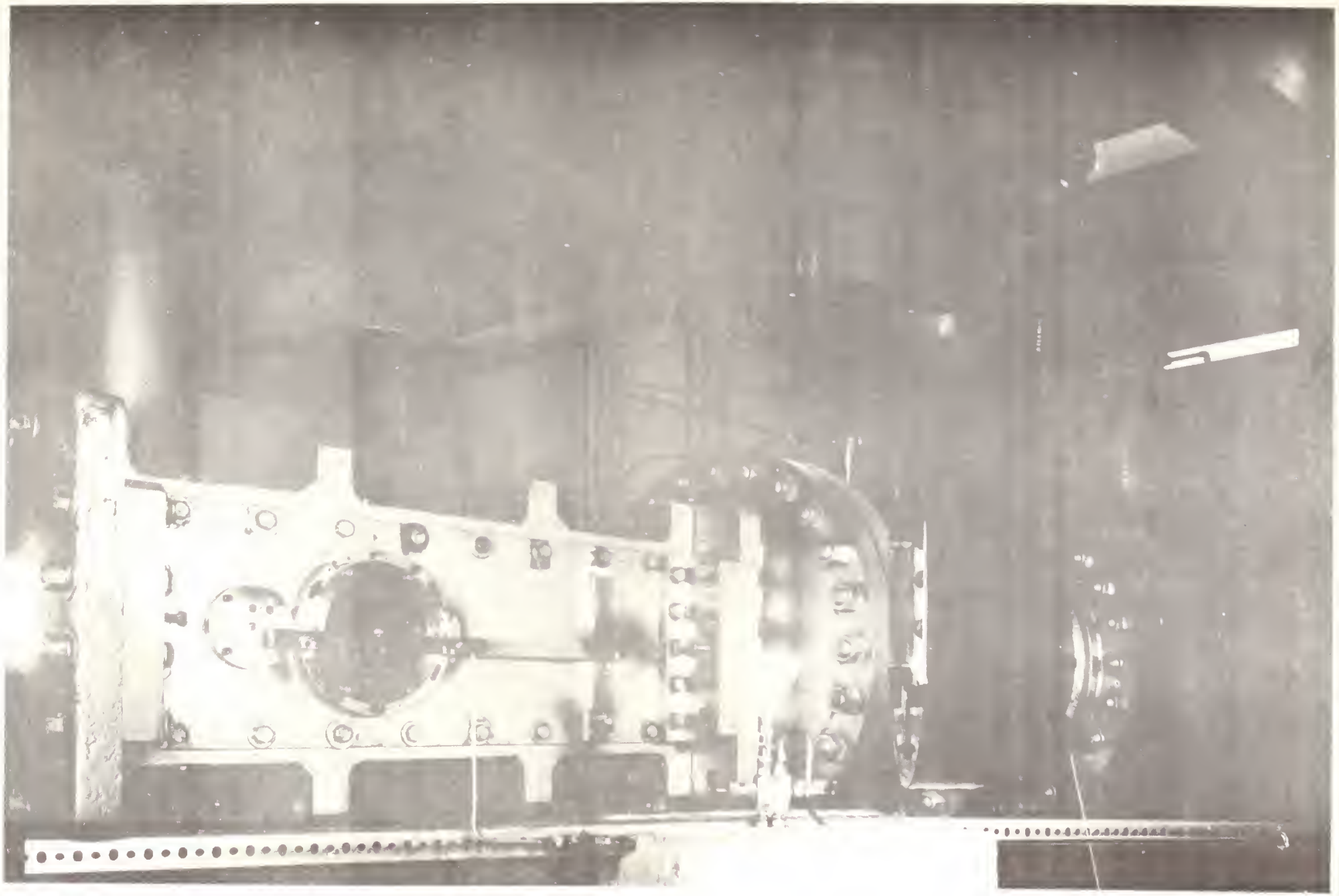


Fig. 6 Photograph of the wind tunnel and injection system installation

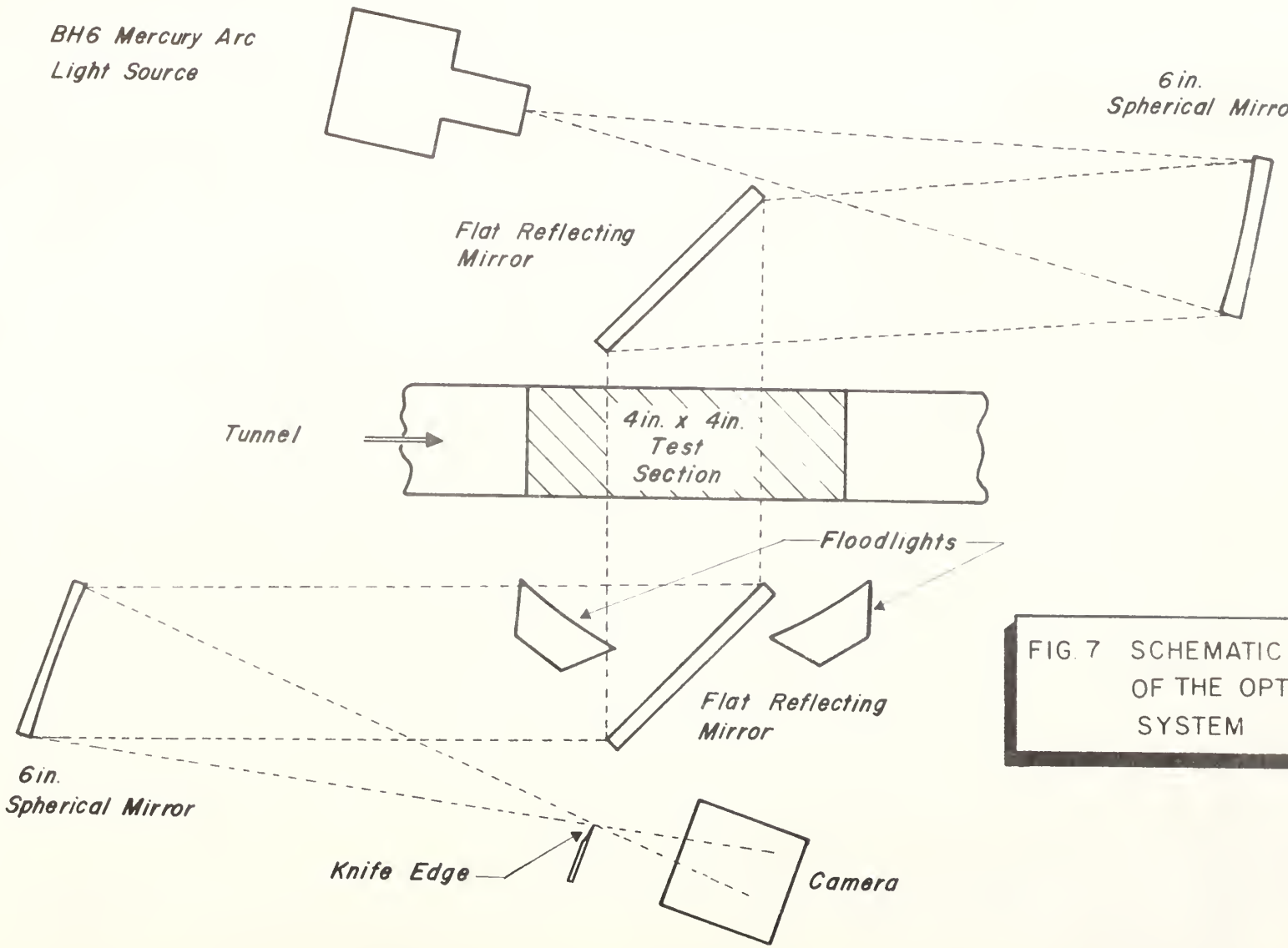


FIG. 7 SCHEMATIC DIAGRAM OF THE OPTICAL SYSTEM

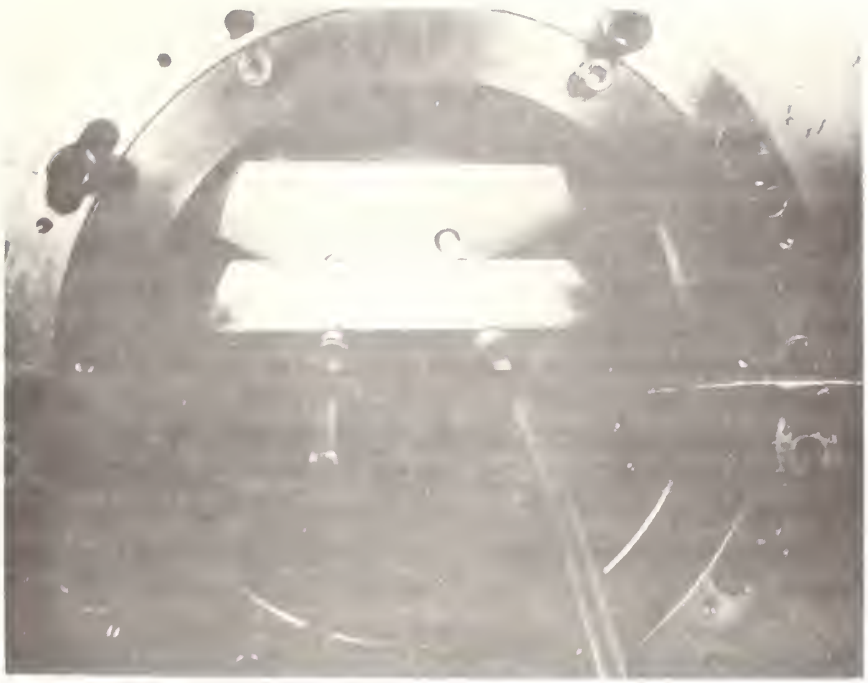


Fig. 8 Photograph of the installation of the penetration flat plate model



Fig. 9 Photograph of the installation of the lateral spreading flat plate model

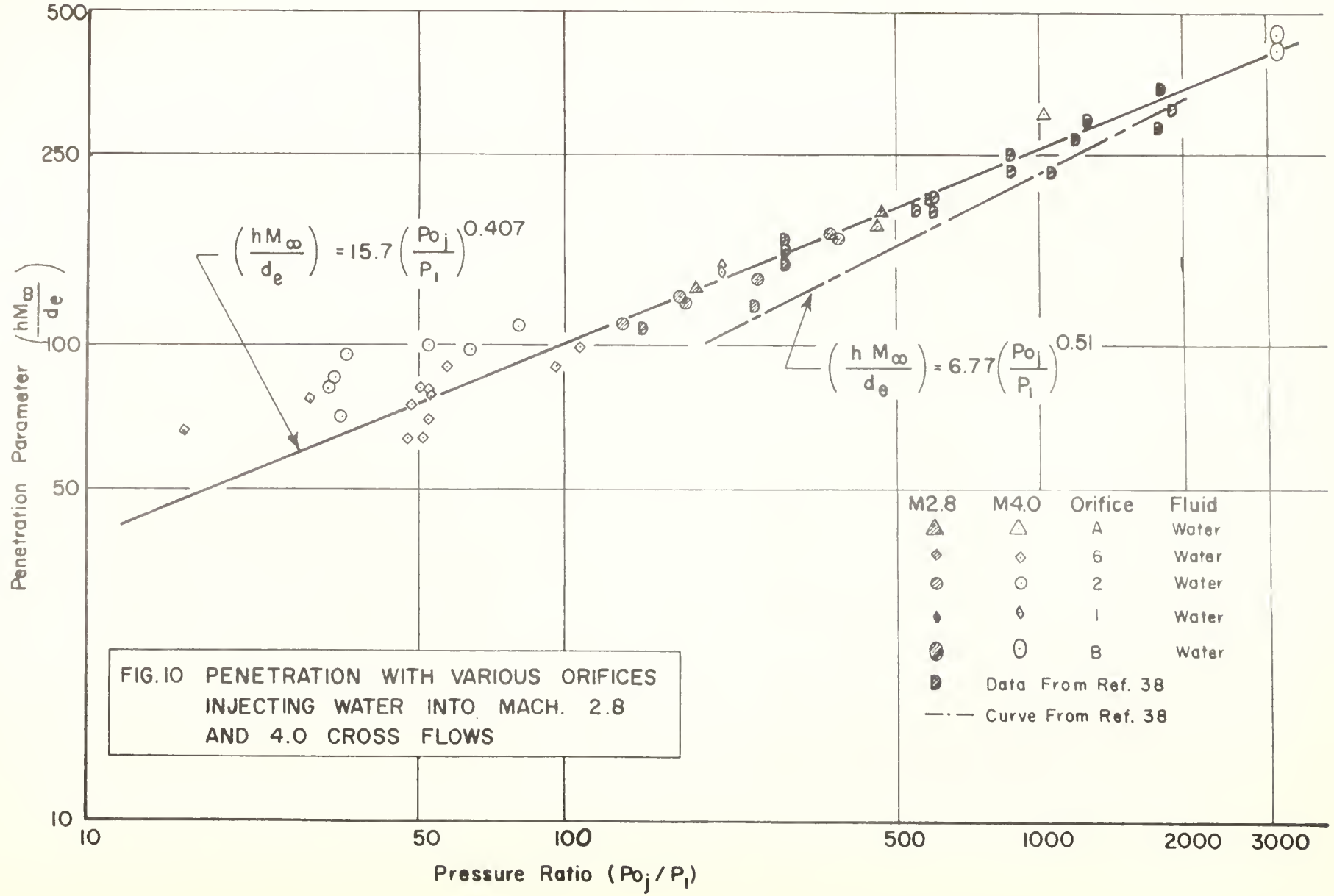


FIG. 10 PENETRATION WITH VARIOUS ORIFICES INJECTING WATER INTO MACH. 2.8 AND 4.0 CROSS FLOWS

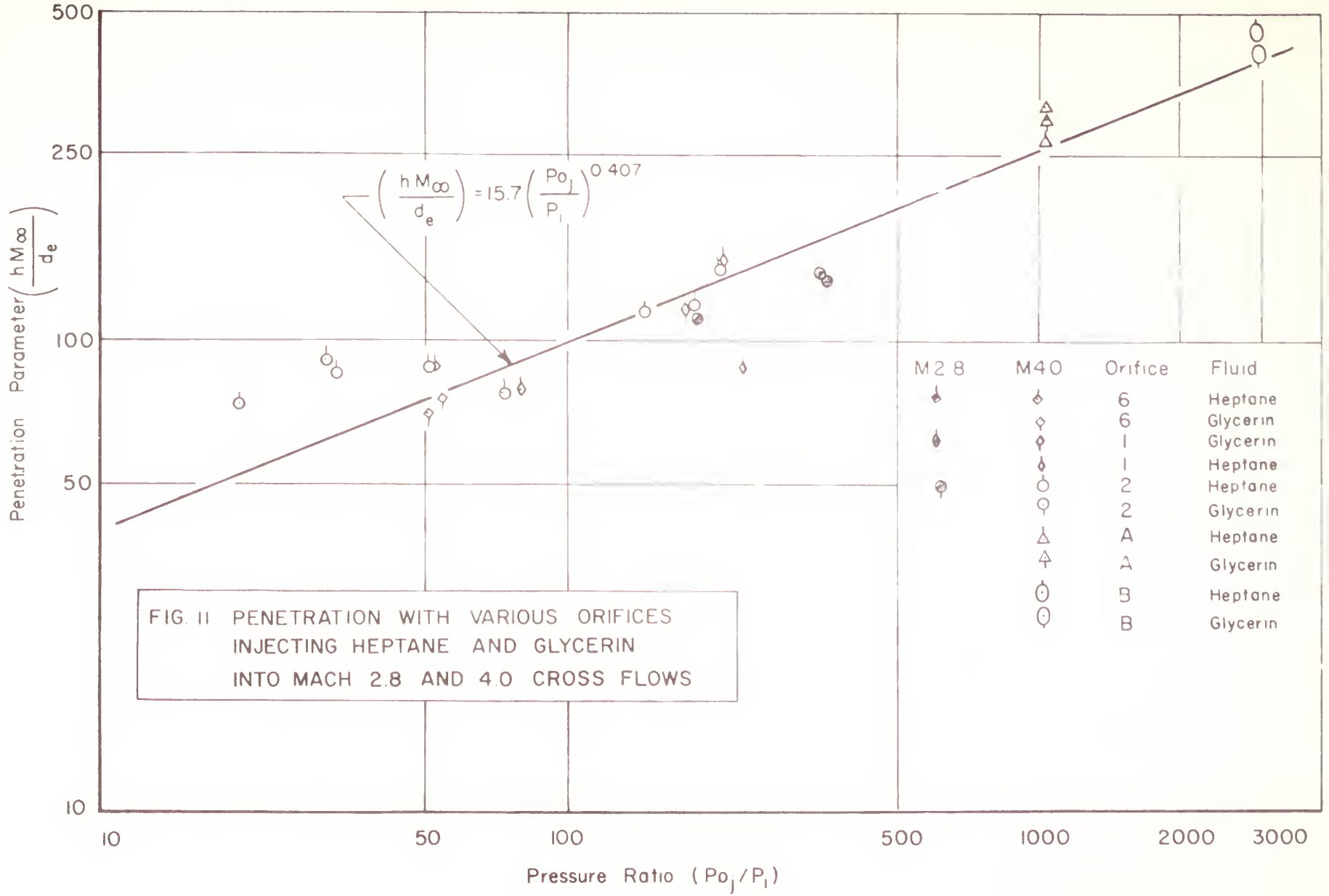


FIG. 11 PENETRATION WITH VARIOUS ORIFICES INJECTING HEPTANE AND GLYCERIN INTO MACH 2.8 AND 4.0 CROSS FLOWS

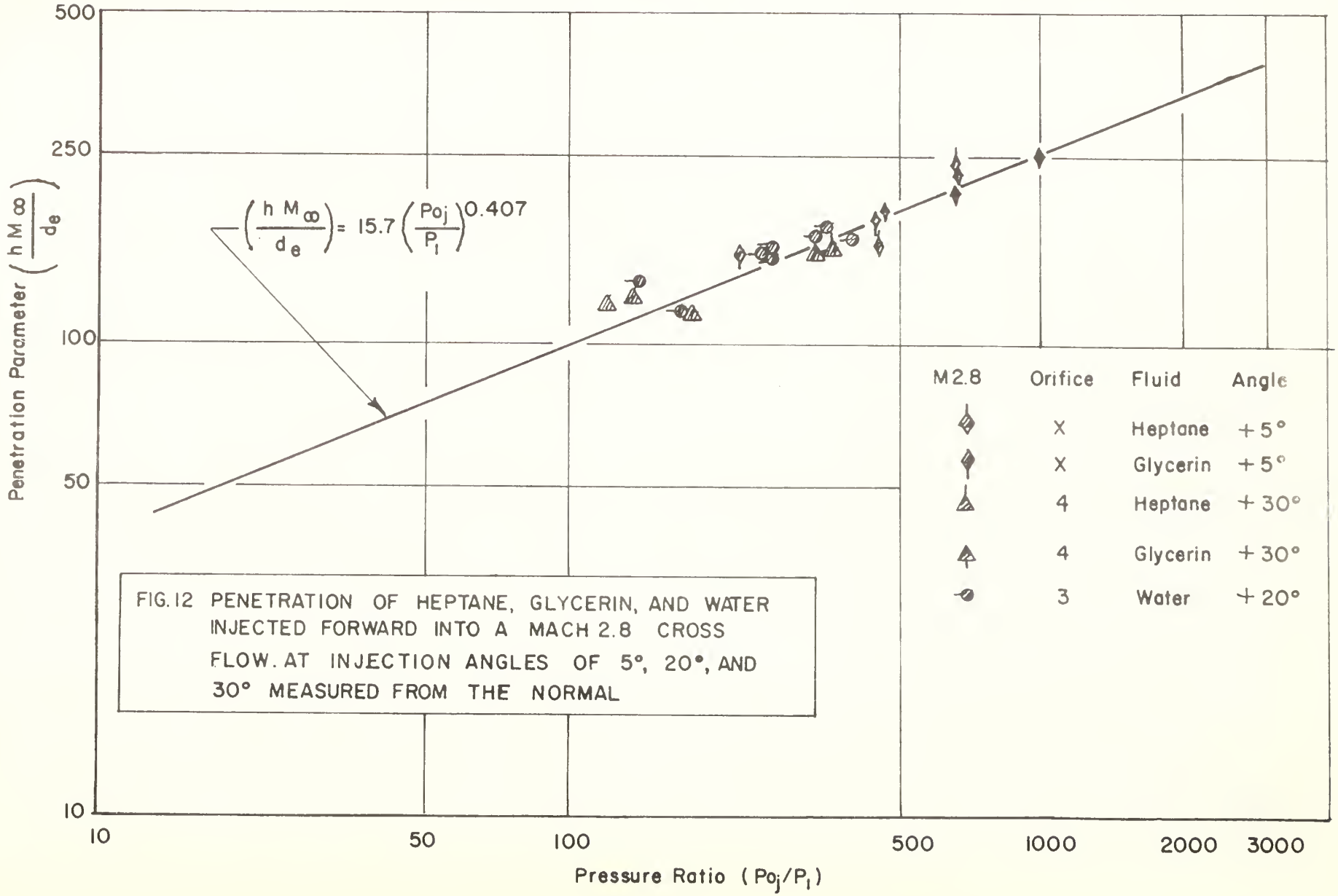


FIG. 12 PENETRATION OF HEPTANE, GLYCERIN, AND WATER INJECTED FORWARD INTO A MACH 2.8 CROSS FLOW. AT INJECTION ANGLES OF 5°, 20°, AND 30° MEASURED FROM THE NORMAL

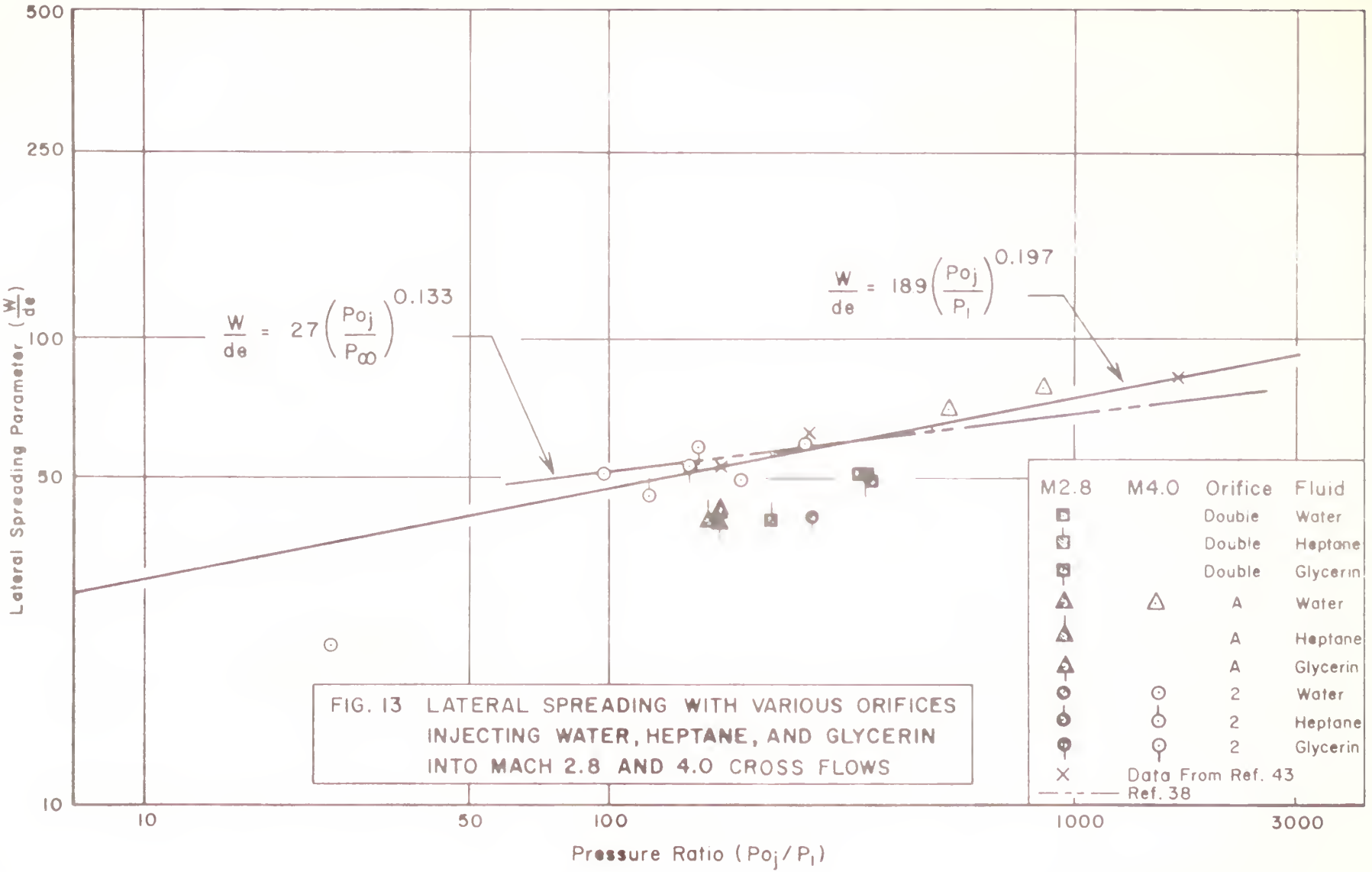


FIG. 13 LATERAL SPREADING WITH VARIOUS ORIFICES INJECTING WATER, HEPTANE, AND GLYCERIN INTO MACH 2.8 AND 4.0 CROSS FLOWS



Fig. 14 Run number 1-3

Fluid - Water	Mach No. 2.8	P_{ot} 114.0 psia.
Injector 2	P_{oj} 750 psia.	P_1 4.18 psia.



Fig. 15 Run number 1-4

Fluid - Water	Mach No. 2.8	P_{ot} 114.7 psia.
Injector 2	P_{oj} 750 psia.	P_1 4.21 psia.



Fig. 16 Run number 1-5

Fluid - water Mach No. 2.8 P_{ot} 80.6 psia.

Injector 2 P_{oj} 400 psia. P_1 2.96 psia.



Fig. 17 Run number 1-6

Fluid - Water Mach No. 2.8 P_{ot} 80.0 psia.

Injector 2 P_{oj} 1100 psia. P_1 2.96 psia.



Fig. 18 Run number 1-7

Fluid - Water Mach No. 2.8 P_{ot} 119.3 psia.

Injector 2 P_{oj} 1570 psia. P_1 4.32 psia.



Fig. 19 Run number 1-8

Fluid - Water Mach No. 2.8 P_{ot} 80.5 psia.

Injector 2 P_{oj} 420 psia. P_1 2.93 psia.







Fig. 22 Run number 1-44

Fluid - Glycerin Mach No. 2.8 P_{ot} 118.9 psia.

Injector 1 P_{oj} 1020 psia. P_1 4.35 psia.



Fig. 23 Run number 1-40

Fluid - Glycerin Mach No. 2.8 P_{ot} 117.9 psia.

Injector 2 P_{oj} 810 psia. P_1 4.34 psia.



Fig. 24 Run number 4-1

Fluid - Water Mach No. 4.0 P_{ot} 144.5 psia.

Injector A P_{oj} 980 psia. P_1 0.95 psia.



Fig. 25 Run number 2-3

Fluid - Heptane Mach No. 4.0 P_{ot} 144.2 psia.

Injector A P_{oj} 990 psia. P_1 0.94 psia.



Fig. 26 Run number 2-4

Fluid - Glycerin Mach No. 4.0 P_{ot} 144.2 psia.

Injector A P_{oj} 1000 psia. P_1 0.94 psia.



Fig. 27 Run number 1-32

Fluid - Water Mach No. 2.8 P_{ot} 61.7 psia.

Injector X P_{oj} 1530 psia. P_1 2.24 psia.

Exp. Time 1/125 sec.



Fig. 28 [illegible]

Fluid - Water [illegible] P_{cf} 61.7 psia.

Injector X [illegible] P_j 2.24 psia.

Exp. Time 1/250 sec.



Fig. 29 [illegible]

Fluid - Water [illegible] P_{cf} 61.8 psia.

Injector X P_{oj} 3500 psia. P_j 2.25 psia.

Exp. Time 1/500 sec.

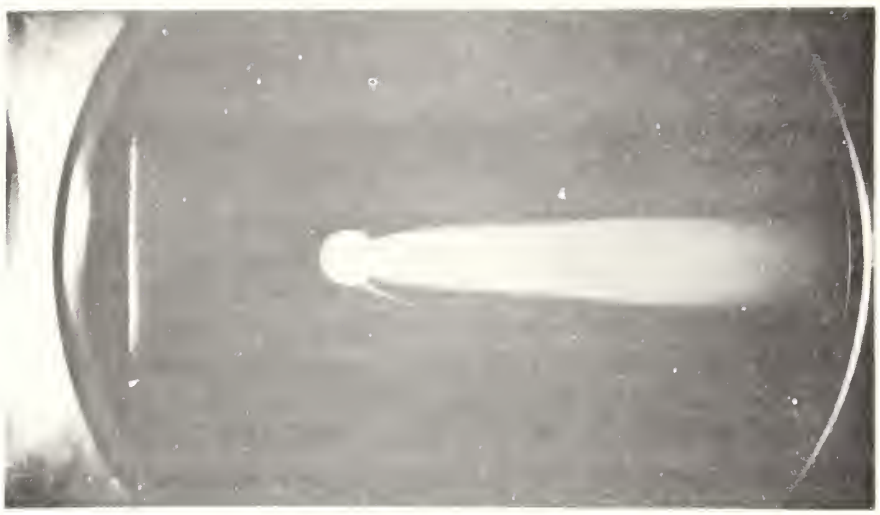


Fig. 30 Run number 1-65

Fluid - Heptane Mach No. 2.8 P_{ot} 119.8 psia.

Injector Double P_{oj} 970 psia. P_l 4.40 psia.



Fig. 31 Run number 1-70

Fluid - Water Mach No. 2.8 P_{ot} 81.5 psia.

Injector A P_{oj} 500 psia. P_l 2.95 psia.

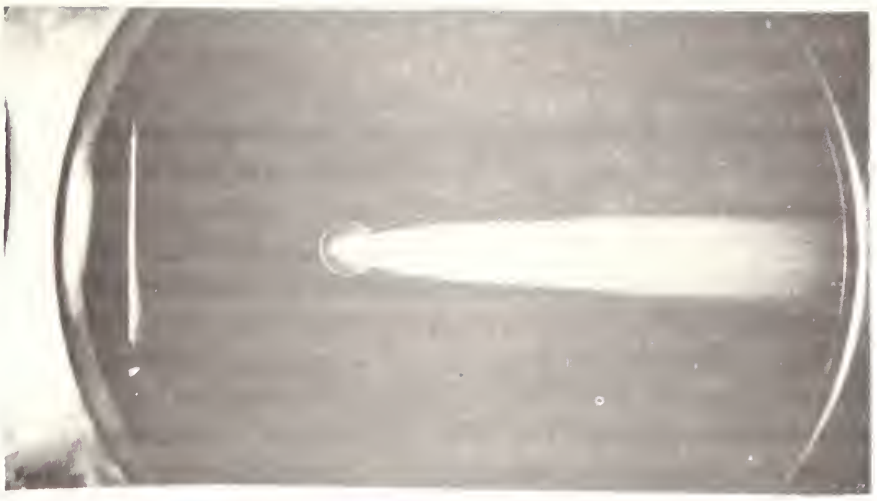


Fig. 32 Run number 1-73

Fluid - Water Mach No. 2.8 P_{ot} 80.9 psia.

Injector A P_{oj} 480 psia. P_1 2.95 psia.

INITIAL DISTRIBUTION LIST

		No. Copies
1.	Defense Documentation Center Cameron Station Alexandria, Virginia 22314	20
2.	Library Naval Postgraduate School Monterey, California 93940	2
3.	Commander, Naval Air Systems Command Navy Department Washington, D. C. 20360	1
4.	Professor R. E. Reichenbach Department of Aeronautics Naval Postgraduate School Monterey, California 93940	5
5.	Chairman, Department of Aeronautics Naval Postgraduate School Monterey, California 93940	10
6.	Professor Allen Fuhs Department of Aeronautics Naval Postgraduate School Monterey, California 93940	1
7.	Dr. K. P. Horn Aerospace Corporation Post Office Box 95085 Los Angeles, California 90045	2
8.	Frederick S. Billig Applied Physics Laboratory Johns Hopkins University Silver Springs, Maryland 20907	1
9.	Mr. B. Drimmer Code 033 Naval Ordnance Systems Command Washington, D. C. 20360	1
10.	Dr. Bernard T. Wolfson Air Force Office of Scientific Research Attn: SREP 1400 Wilson Boulevard Arlington, Virginia 22209	1
11.	Professor David Wooten Department of Aeronautics Naval Postgraduate School Monterey, California 93940	1

		No. Copies
12.	Mr. Ted Dunton Department of Aeronautics Naval Postgraduate School Monterey, California 93940	1
13.	Mr. Norman Leckenby Department of Aeronautics Naval Postgraduate School Monterey, California 93940	1
14.	Professor D. J. Collins Department of Aeronautics Naval Postgraduate School Monterey, California 93940	1
15.	LT Robert Wellington Castle Jr. Attack Squadron 122 Naval Air Station Lemoore, California 93246	3

DOCUMENT CONTROL DATA - R&D

(Security classification of title, body of abstract and indexing annotation must be entered when the overall report is classified)

1 ORIGINATING ACTIVITY (Corporate author)

Naval Postgraduate School
Monterey, California 93940

2a REPORT SECURITY CLASSIFICATION
Unclassified

2b GROUP

3 REPORT TITLE

AN INVESTIGATION OF PENETRATION AND SPREADING FOR VARIOUS FLUIDS INJECTED INTO A SUPERSONIC STREAM

4 DESCRIPTIVE NOTES (Type of report and inclusive dates)

5 AUTHOR(S) (Last name, first name, initial)

Robert Wellington Castle, Jr.
Lieutenant, U. S. Navy

6 REPORT DATE	7a TOTAL NO. OF PAGES	7b NO. OF REFS
March 1968	75	44

8a CONTRACT OR GRANT NO

b PROJECT NO

c

d

9a ORIGINATOR'S REPORT NUMBER(S)

9b OTHER REPORT NO(S) (Any other numbers that may be assigned this report)

10 AVAILABILITY/LIMITATION NOTICES

[redacted]

11 SUPPLEMENTARY NOTES

12 SPONSORING MILITARY ACTIVITY
Naval Postgraduate School
Monterey, California 93940

13 ABSTRACT

A study was conducted to determine the effects of varying the fluid properties of viscosity, surface tension, and density on liquid jet breakup, penetration, and spreading. Water, heptane, and a 58 per cent glycerin-42 per cent water mixture (by mass) were injected transversely into Mach 2.8 and 4.0 airstreams through various circular orifices located in the surface of a flat plate model. Experiments were performed with injector orifices varying in diameter from 0.0145 inches to 0.080 inches, using injectant total pressures ranging from 30 psia. to 3000 psia. Steady-state penetration and lateral spreading distances were measured from scattered light photographs, and qualitative analyses of shock waves induced by the liquid jet were made using schlieren photographs.

A non-dimensional penetration parameter ($M_\infty h/d_e$) was found to be dependent on the ratio of the injection total pressure to the free stream static pressure, but not on a variation of fluid injectant properties of surface tension, viscosity, and density.

Lateral spreading was determined to be a function primarily of the orifice diameter, with weak dependence upon the injection pressure ratio. Changing the injectant fluid properties of surface tension, viscosity, and density had no noticeable effect on lateral spreading. Within experimental accuracy, spreading was also considered to be Mach number independent.

DD FORM 1 JAN 64 1473

14 KEY WORDS	LINK A		LINK B		LINK C	
	ROLE	WT	ROLE	WT	ROLE	WT
Fluid Injection						
Liquid Injection						
Supersonic Injection						



thesC325
DUDLEY KNOX LIBRARY
3 2768 00407873 3
DUDLEY KNOX LIBRARY